

Contents lists available at ScienceDirect

Transportation Research Part B

journal homepage: www.elsevier.com/locate/trb





Robust and resilient equilibrium routing mechanism for traffic congestion mitigation built upon correlated equilibrium and distributed optimization

Yuqiang Ning, Lili Du

Department of Civil & Coastal Engineering, University of Florida, 518b Weil Hall, Gainesville, FL 32611

ARTICLE INFO

Keywords: Equilibrium routing mechanism Correlated equilibrium Distributed algorithm Robust and Resilient algorithm Online traffic routing Congestion mitigation

ABSTRACT

With the rapid development of wireless communication, mobile computing, and GPS technologies, drivers' route decisions nowadays rely more on navigation services, such as Google or Waze. However, these navigation services don't always come with improved traffic conditions. Individual drivers often make independent and selfish route decisions that are not systematically favorable and thus often result in severe congestions. This study aims to alleviate such problems by exploiting the information gaps between individuals and the central planner (CP). Specifically, we develop a correlated equilibrium routing mechanism (CeRM) for the CP, which drives a group of vehicles' route choices to an equilibrium with a systematically optimal traffic condition while still satisfying individuals' selfish nature. Participating drivers would only be better off by following the suggested routing guidance than navigating on their best responses to real-time traffic information. The CeRM is modeled as a nonconvex and nonlinear program involving a large-scale of users. A distributed Augmented Lagrangian algorithm (D-AL) is developed to efficiently solve the CeRM to provide online real-time navigation service, taking advantage of the onboard computation resources of individual vehicles. Considering the D-AL relies on the wireless communications between vehicles and the CP, we proved the convergence robustness of the D-AL against random communication failures and derived the convergence rate upper bound as a function of the communication failure probability. It is noticed that the convergence rate of the D-AL degrades dramatically as the communication failure probability increases, which hampers the applicability of implementing the CeRM in practice. To improve the solution algorithm's resilience in the computation performance, we further designed and proved an acceleration scheme aided D-AL (aD-AL) to expedite the convergence rate under the high likelihood of communication failures. Numerical experiments conducted on the Sioux Falls city network confirmed the D-AL's convergence properties, robustness against random communication failures, and the resilience of the aD-AL to solve the CeRM. The experiments also show that the CeRM results in better system performance (have less system cost) compared with the existing Independent Routing (IR) mechanism and user-oriented Equilibrium Routing (uoER) mechanism.

E-mail address: lilidu@ufl.edu (L. Du).

^{*} Corresponding author.

1. Introduction

Traffic congestion has long been a major issue in urban areas, which happens when the demand is higher than road capacity. With the development of mobile intelligent devices and wireless communication technologies, drivers nowadays rely heavily on traveler information systems (TIS) such as Google Maps, Apple Maps, and Waze to get real-time traffic information and make their best response to avoid congestion. This study refers to this widely used routing mechanism as Independent Routing (IR). However, if too many vehicles simultaneously choose similar routes/links according to the same provided information, these recommended routes/links would become congested later. This phenomenon resulting from the collective snapshot routing decisions of drivers relying on IR is known as the flash crowd effect (Grzybek et al., 2015), which may cause severe traffic congestion and incur high system costs for all drivers. On the contrary to IR, System Optimum routing (SOR) seeks to minimize the total travel cost of all drivers, which is the ideal traffic state that a system wants to achieve. However, SOR will sacrifice some users' interest (experience more travel costs) in exchange for better system performance, which conflicts with individuals' selfish nature. In addition, the computation load to implement real-time SOR is prohibitive.

Transportation researchers have long been devoted to developing navigation systems for reducing traffic congestion and pushing the routing pattern to be more systematically efficient. One of the most widely studied approaches is congestion pricing. Along with its variants like credit- or permit-based regulations, congestion pricing influences the behavior of individuals by changing their perceived cost physically/monetarily. Interested readers can refer to (de Palma and Lindsey, 2011; Lessan and Fu, 2019) for a comprehensive review. While theoretically, congestion pricing could push the traffic state close to system optimal and is undoubtedly a powerful tool to improve traffic conditions in practice, the study of (de Palma and Lindsey, 2011) summarized seven main complications when implementing congestion pricing. Along with social equity, fairness, legislature, and political issues, congestion pricing still has obstacles to address in practice, and researchers are thus motivated to explore alternative options (Klein, Levy, and Ben-Elia, 2018; Menelaou et al., 2017; Menelaou et al., 2018; Rey et al., 2016).

Several recent studies (i.e., (Du, Han, and Li, 2014; Du, Chen, and Han, 2015; Grzybek et al., 2015)) proposed a different routing approach based on snapshot equilibrium routing (ER) to mitigate traffic congestion and improve traffic conditions. Mainly originating from game theory in economics, ER aided by real-time traffic information is a class of emerging routing mechanisms that try to manipulate individual drivers' real-time route choices to approach a snapshot equilibrium by coordination or information provision technologies (discussed in detail in the literature review). To be noted, the collective snapshot routing decisions relying on IR do not lead to such snapshot route choice equilibrium. Therefore, ER seeks to reduce traffic congestion by mitigating the flash crowd effect resulting from the over-competition on the provided shortest paths, often observed in IR. In addition, unlike compulsive law enforcement or congestion pricing, ER influences individuals' perceptions and decisions without using external regulation and incentives, thus avoiding many impedances faced in typical road pricing schemes. However, though ER could reduce system costs compared with IR, most existing ER mechanisms are still away from SOR since they are still user-oriented, and system interest (system optimality) is only implicitly considered by the routing mechanism design. We categorize this type of ER as user-oriented ER (uoER).

In short, IR is a snapshot collective routing decision of all travelers, in which each traveler takes the best response to the real-time traffic information provision and won't reach an equilibrium. While uoER is a snapshot routing solution in which participating individual vehicles reach an online user-oriented equilibrium routing decision through a certain routing coordination mechanism (Du, Han, and Chen, 2015; Du, Han, and Li, 2014; Grzybek et al., 2015; Zhou et al., 2020). Though the equilibrium condition of a pure strategy uoER (or mixed strategy uoER) is similar to the user equilibrium condition (or stochastic user equilibrium condition) (Du, Han, and Li, 2014), uoER are atomic routing mechanisms and are essentially different from non-atomic games used by traffic assignments. The difference between the atomic routing mechanisms and traffic assignment problems poses unique research challenges, which will be further discussed in the literature review in Sec 1.2.

Motivated by the above views, this study seeks to go one step further and design an equilibrium routing mechanism toward a better system performance than uoER. Specifically, this study develops a Correlated equilibrium online routing mechanism (CeRM) based on correlated equilibrium and robust distributed solution algorithm. The CeRM generates a snapshot routing solution in which participating individual vehicles reach a Correlated equilibrium (CE) that minimizes the system cost. The CeRM drives the traffic state to a CE constrained system optimum that outperforms existing uoER. In addition, the CeRM does not violate individuals' selfish nature, and thus drivers would be willing to follow the proposed routing decision. Ranking the routing mechanisms' efficiency regarding system performance, we will have $IR \le uoER \le CeRM \le SOR$.

The idea of developing such an ER using correlated equilibrium is invoked by exploiting the information discrepancies between individual drivers and the central planner (CP) in existing route navigation systems. Specifically, in a navigation scenario, each driver only knows their own trip information but has no idea of others, e.g., how many travelers are there on the road, where they are going, their personal choice characteristics, etc. The lack of panoramic information at the individual level makes drivers unable to know/predict traffic conditions in the future and often make the best response to the real-time traffic information provided by the navigation service. On the other hand, the CP is omniscient and could better predict traffic conditions in the near future since it can get comprehensive information by collecting travelers' trip plans when they require navigation services. Such an information gap allows the CP to act as a trusted agent, which can strategically design and provide individual drivers with route choices that no one would want to deviate from. Correspondingly, this study develops the CeRM, which calculates and suggests each traveler's routing preferences according to their trip features (mainly origins, destinations, and personal choice characteristics), aiming to achieve the desired system optimal performance while guaranteeing that an individual driver would not be better off if they unilaterally deviate from the suggested routing preferences (i.e., correlated equilibrium).

Moreover, to satisfy the computation need of online navigation services, this study develops a distributed and robust solution

algorithm (D-AL). It distributes the computation load of searching a correlated equilibrium route decision to individual vehicles' onboard computing devices. The D-AL relies heavily on wireless communications for transmitting data/information between vehicles and the Central Planner (CP), which happens to be unstable in real-world applications due to poor network conditions and/or vehicle on-board devices malfunctioning. In view of this implementation issue, this study proves that the D-AL is robust to random communication failures, but its convergence rate will be affected. Built upon these results, we further provide an acceleration scheme (aD-AL) to expedite the convergence speed and improve the solution algorithm's resilience in the computation performance against communication failures.

Overall, this study has four distinguished characteristics and methodology contributions:

- (i) Taking advantage of the information discrepancies, we developed a Correlated equilibrium Routing Mechanism (CeRM) built upon a mixed strategy atomic game using correlated equilibrium to coordinate individual travelers' real-time routing decisions, which push traffic conditions toward a desired system optimal performance without introducing external regulation and incentives.
- (ii) To serve a large-scale of travelers' online navigation requests, we developed a problem-specific robust and distributed solution algorithm (D-AL) by taking advantage of the model's unique structure features. The D-AL could solve the CeRM problem efficiently by distributing the computation load to individual vehicles' onboard computing devices.
- (iii) Considering the D-AL relies on wireless communications between vehicles and the CP, we proved the convergence robustness of the D-AL against random communication failures and derived the convergence rate upper bound as the function of communication failure probabilities.
- (iv) By recognizing that the probability of communication failures would slow down D-AL's convergence rate, we further designed an acceleration scheme aided D-AL (aD-AL) to expedite the convergence rate and improve the solution algorithm's resilience in the computation performance under high likelihoods of communication failures.

Last, the numerical experiments validate our solution algorithms' computation performance, robustness, and resilience properties and demonstrate that the CeRM could reduce traffic congestion and system cost compared with existing IR and uoER. More exactly, our experiments show that the CeRM can significantly reduce traffic congestion and system travel time by 55% and 3.6% compared to the existing IR and uoER mechanisms. The D-AL could handle a scenario with more than a thousand vehicles by a leading time smaller than 22 seconds and could converge under different probabilities of random communication failures. The experiments also confirm that the aD-AL could expedite the convergence rate under the high likelihood of communication failures.

To the best of our knowledge, this is the first research to design a correlated equilibrium routing mechanism with an efficient and robust solution algorithm to mitigate traffic congestion and reduce the system cost. We are also among the pioneer studies to investigate the routing mechanism against communication failures. It significantly contributes to the methodology development and practice for the field of traffic congestion mitigation.

The rest of the paper is organized as follows. Section 2 reviews relevant works in the existing literature and identifies the research gaps this study addresses. Following that, we introduce related notations and concepts in section 3, and then design the correlated equilibrium routing scheme in section 4. Section 5 develops an effective distributed solution algorithm and theoretically discusses its robustness and convergence properties. We demonstrate the efficiency and efficacy of the proposed routing scheme and solution algorithm through the numerical experiments in section 6. Last, section 7 concludes the whole paper. We will use "vehicle" and "driver" interchangeably in the following context for better illustration.

2. Literature Review

This study aims to develop a correlated routing mechanism by exploiting the information gap between drivers and the CP, which could reduce congestion at the system's level while still maintaining individuals' selfish nature. In literature, this research sits in the field of flash crowd effect, equilibrium routing, correlated equilibrium, and information design. This section will briefly review some of the most relevant works to our study and identify their research gaps.

We first recognized the studies in the field of the price of anarchy, which measures and mitigates the inefficiency of selfish routing in user equilibrium traffic assignment. In the transportation field, the price of anarchy (Koutsoupias and Papadimitriou, 1999; Roughgarden, 2005) refers to the degradation of system performance due to selfish routing, which is measured as the worst-case ratio between the cost of a flow at user equilibrium (first Wardrop Principle) and that of system optimum/second Wardrop Principle. The bound of the price of anarchy has been studied by a series of works in different network topologies, different types of cost functions, and different types of games (atomic or non-atomic). There are different strategies used to mitigate the price of anarchy, including network designs, centrally controlled traffic, congestion pricing, system traffic assignment with user constraints, etc. Interested readers can refer to the seminar book (Roughgarden, 2005) for a comprehensive review. The studies that improve system performance by congestion pricing and its variants like credit- or permit-based regulations have been credited and briefly introduced in the Introduction section. Considering these studies mainly focus on imposing and designing physical externalities such as toll pricing, which is different from our study that focuses on designing information provision (i.e., the suggested route preference) to affect route choices and form ER, the following survey does not provide detailed reviews for their methodology development. Interested readers can refer to (de Palma and Lindsey, 2011) and (Koutsoupias and Papadimitriou, 1999) for a comprehensive review. The studies in system optimal traffic assignment with user constraints will be reviewed and discussed later in this section.

We also recognized the studies of Pareto-improvement problems in routing games (Guo and Yang, 2010; Klein, Levy, and Ben-Elia,

2018; Simon, 1955). It shares similar thoughts to this study since it benefits at least one vehicle without harming anyone. However, most existing studies working on Pareto-improvement problems in routing games rely on exploring optimal congestion pricing and tolls to reach a solution, which differs from the focus of this study that guides travelers' route preferences to reach an equilibrium decision by designing information provision strategies (i.e., without using externalities). Therefore, we do not provide comprehensive discussions of their methodologies in this review.

In literature, the flash crowd effect (Grzybek et al., 2015), also known as overreaction (Ben-Akiva, Palma, and Isam, 1991), occurs in traffic when a large number of drivers receive similar traffic information and make routing decisions based on it selfishly and independently. Different ER mechanisms have been proposed to mitigate such adverse phenomena in either distributed or centralized ways. In (Du, Han, and Li, 2014), the author developed an online coordinated routing mechanism based on an atomic mixed strategy congestion equilibrium. By iteratively sharing and updating the routing preference for each vehicle, the coordinated routing mechanism guarantees to converge to an equilibrium routing decision which leads to better system cost than the IR mechanism. On the other hand, (Grzybek et al., 2015) proposed to perform route selections centrally. Vehicles are assigned to suggested routes with probabilities calculated by the central server. The probability is inversely proportional to the estimated travel time, and the resulting routing decision avoids the situation that a large number of vehicles choose the same route. There are many other approaches to deriving an ER, and most of them share similar thoughts with (Grzybek et al., 2015) and (Du, Han, and Li, 2014). For example, (Du, Chen, and Han, 2015) conducted the coordinated routing under the pure strategy setting, (Zhou et al., 2020) proposed to solve the mixed strategy coordinated routing problem similar to (Du, Han, and Li, 2014) using the reinforcement learning method, and (Mahajan et al., 2019) proposed an anticipatory navigation service that predicts and disseminates the near future traffic condition based on real-time data. While simulation results show that all these approaches could reduce the system cost compared with IR, their performance is still away from SOR. This is because the routing decision in uoER can be considered a spontaneous equilibrium resulting from drivers' selfish reactions to perfect traffic information. Though certain mechanism designs of uoER could mitigate the overreaction of drivers' routing decisions, the resulting system cost is still sub-optimal compared with SOR since there are conflicts between user performance and system performance. The CeRM proposed in this study falls into the category of ER but differs from existing uoER in that it explicitly incorporates system cost minimization in the routing mechanism design.

Another research area that shares similar thoughts to our study in literature is system optimal traffic assignment with users' constraints. They conduct system optimum traffic assignment under the consideration of user fairness and cooperation willingness. The approaches used in this field can be divided into two branches. One incorporates users' fairness constraints in the system optimum to stabilize the resulting system optimum flow. The other relaxed the user equilibrium condition to improve the system performance of user equilibrium flows. Interested readers can refer to (Morandi, 2021) for a detailed review. Though these studies achieve further system cost reduction without using externalities in road pricing schemes, they are different from our work in four aspects.

Firstly, traffic assignments modeled using non-atomic games do not fully take into account the heterogeneities of individual travelers' characteristics, since they usually consider user classes (i.e., aggregated traffic flow) and neglect the behavioral and response differences among the individuals within a user class (within traffic flow). Our CeRM, due to travelers' unique characteristics, allows individual travelers even belonging to the same OD pair within the same class to have different candidate paths, take different paths, or have different priorities for their candidate paths.

Secondly, the user constraints adopted in the area of system optimal traffic assignment with user constraints mainly focus on bounding a certain level of unfairness imposed on individual vehicles. It aims to reduce the system cost by sacrificing a little (experiencing a bounded amount of longer travel distance or travel time) for some drivers. This may raise compliance issues since it is not completely fair and will raise the issue like who will be sacrificed. On the contrary, our CeRM involves a Correlated equilibrium condition to ensure user compliance. Given the individual's limited information provision (only knows the real-time traffic condition), the Correlated equilibrium ensures that every participating vehicle will experience less travel cost by following the routing suggestion. Thus, along with the heterogeneities issue, our CeRM carries more realities for real-time in-vehicle route navigation that the traffic assignment models usually neglect for traffic planning purposes.

Thirdly, the CeRM targets a real-time application involving a large scale of travelers differentiated by their unique candidate routes and choice behavior. This particular application raises unique computation challenges compared with the traffic assignment for traffic planning purposes. Along with that the user constraints in our CeRM are quite different from models in the constrained system optimal traffic assignments, existing solution algorithms developed for traffic assignment models cannot efficiently solve the CeRM with an applicable computation performance. Fourthly, from the implementation point of view, the CeRM will serve travelers through a service app on each user's mobile device and its communication to a server. Thus, it is a distributed system involving a large scale of independent agents. The centralized computation is very unlikely to satisfy this application. This study thus proposes the distributed solution algorithm by taking advantage of the local computation resources of each mobile device and the wireless communication technology. This in turn raises new challenges in dealing with unstable wireless communications between vehicles and the CP and motivates us to study the robustness and resilience of the distributed solution algorithm in our CeRM.

Recently, (Du, Han, and Chen, 2015) and (Spana, Du, and Yin, 2021) proposed to improve the performance of uoER by providing a perturbed travel time to drivers in the navigation service. Mainly, this study seeks to manipulate individual drivers' real-time route choices toward a better system performance by strategically involving bias in travel time provision. While this approach could reduce the system cost and rational drivers are likely to comply, it may induce fairness issues. Specifically, some drivers responding to perturbed traffic information may experience a sacrifice in travel time compared with responding to unperturbed traffic information. In comparison, in our work, we propose to reach a systematically efficient equilibrium routing decision based on the naturally existing information gap between drivers and the central planner. The proposed CeRM guarantees that every driver would be better off (at least not worse off) given their limited individual information and thus precludes the issue of individual fairness.

The method in this study is built upon the correlated equilibrium (CE). In literature, CE often relates to the field of information design and Bayesian Persuasion. These studies particularly developed for the transportation system aimed to find out how a central planner can design an information structure to induce a preferred traffic state. By designing the informational environment, the planner can manipulate the individual's behavior and direct the resulting equilibrium to serve its own interests. Even though information and CE have great potential to improve the system performance without using externalities, it is still an emerging area in the transportation field and has many opening research questions not been solved. For example, the study of (Gairing, Monien, and Tiemann, 2008) proposed a general framework that modeled selfish users with incomplete information as a Bayesian routing game. The study proved the existence of correlated equilibria in the routing game and analyzed the computation complexity and the bounds of the price of Anarchy. However, the study is built upon simple networks with parallel and identical links. In addition, developing a practical solution algorithm to solve such models is not the focus of this study. (Ma, Smith, and Zhou, 2016) built an agent-based optimization model that provides partial information for drivers to improve traffic congestion. In their routing scheme, the CP designs how many drivers and which drivers will receive the broadcast of information about traffic accidents on routes. However, their study considered constant travel time under normal traffic conditions, thus ignoring the interaction between traffic flow and congestion. Also, the proposed solution method took several hundred seconds to solve cases with only 300 vehicles. This computation performance is not efficient enough for an online navigation service. (Tayafoghi and Teneketzis, 2017) provided a private information disclosure mechanism to guide individual drivers to obtain a better social objective, Compared with (Ma, Smith, and Zhou, 2016), drivers in this work have ex-ante expectations about the probability of an accident but do not know what exactly happens. They proved that disclosing all information (whether there is an accident or not) publicly to every driver is less optimal than disclosing partial or manipulated information. Several researchers have conducted similar studies, e.g., (Das, Kamenica, and Mirka, 2017; Liu, Amin, and Schwartz, 2016; Lotfi, La, and Martins, 2018). However, these studies all used simplified to parallel two-link networks and ignored the effect of congestion brought by the increasing number of drivers. (Liu and Whinston, 2019) theoretically studied the correlated equilibrium on a two-link network and then extended to multi-link non-parallel networks, considering the congestion effect. The study considered that drivers knew the probability of traffic flow on the road, while the CP knew the realization of traffic flow. Though shared the same interest, our study considers different information discrepancies focusing on travelers' route choice preferences. More exactly, we assume drivers are informed of real-time traffic information and would make the best response, while the CP can collect and aggregate travelers' route choice intentions and predict future traffic conditions. This difference in the definition of the information discrepancy leads to very different formulations and associated research challenges. In addition, most existing efforts that studied information design/Bayesian Persuasion/Correlated equilibrium in routing problems focused on modeling and analyzing their impacts. To the authors' best knowledge, there is no existing work providing efficient solution algorithms to solve these problems for online navigation services.

To conclude, the state of the art indicates two major research gaps. 1) Most existing ER mechanisms do not completely address the inefficiencies brought by the conflicts between individual performance and system performance or user compliance issues. 2) Existing CE research in routing problems can be further improved by involving realistic transportation network modeling and practical solution algorithms. This study seeks to partially fill such research gaps by involving these enhanced features and addressing the new research challenges. Briefly, this study develops a CE-based ER mechanism (i.e., CeRM), which reduces system cost compared with uoER and satisfies individuals' selfish nature using a different line of approach from congestion pricing. Briefly, the CeRM is built upon a transportation network with multi origin-destinations, multi-link non-parallel routes, and well-accepted link cost functions. To adapt this CeRM to the online application, we develop a distributed solution algorithm and prove it to be efficient and robust for real-world scenarios with thousands of vehicles opting in the services. The following sections introduce the technical details for developing the CeRM.

3. Preliminary

This section will first introduce some mathematic notations and the concept of correlated equilibrium and then propose the correlated equilibrium routing mechanism in section 4.

3.1. Mathematic notations

Denote G = (N, L) to be the directed graph of a transportation network, where N is the set of nodes and L is the set of arcs (links). Let v = 1, ..., m be the qualified vehicle on roads. Each vehicle v has a specific origin-destination (OD) pair $(o_v, d_v) \in N \times N$ and a set of k_v possible routes. Denote r_v^i as the ith possible route of vehicle v, where $i = 1, ..., k^v$. This study uses the mixed strategy to account for the stochastic choice behavior of travelers, in which the travelers' perceived utilities are influenced by uncertainties and are not deterministic. In the mixed strategy setting, every player places a probability distribution (i.e., preference) on their set of available choices. In the routing problem, each vehicle is a player, and their possible paths are potential alternatives. Denote $p^{v,i}$ as the probability that vehicle v places on the route v_v^i . Then clearly, we have

$$\sum_{i=1}^{k_{\nu}} p^{\nu,i} = 1, \ \forall \nu = 1, ..., m.$$
 (1)

The probability $p^{v,i}$ can also be viewed as the expected volume generated by vehicle v on route r_v^i . Thus, we could form the expected flow on link l as

$$f^{l} = \sum_{\nu=1}^{m} \sum_{i=1}^{k^{\nu}} p^{\nu,i} \delta_{\nu,i}^{l}, \tag{2}$$

where the link-route incidence indicator $\delta_{v,i}^l = 1$ if link l is used by route r_v^i , and 0 otherwise. Associated with each link is a link travel cost $c_l(f_l)$. Then, for each route i of vehicle v, a generalized travel cost C_v^i could be defined.

$$C_{v}^{i}(\mathbf{P}) = \sum_{l \sim v, i} c_{l}(f^{l}), \tag{3}$$

where P is the set of all vehicles' route choice preferences, i.e., $P = \{p^{v,i}\}, v = 1, ...m, i = 1, ...k^v$. This study models the uncertainties in the traveler's stochastic choice behaviors by the well-accepted multinomial logit choice model. Denote the current (initial) travel time on route i of vehicle v as $C^i_{v,o}$. Then according to $C^i_{v,o}$, individual vehicle's selfish route choice preference could then be calculated by a multinomial logit (MNL) choice model:

$$p_o^{v,i} = \frac{e^{V_{v,i}}}{\sum_{i=1}^{k^v} e^{V_{v,i}}},\tag{4}$$

Where

$$V_{v,i} = -\left(\alpha^{v} + \beta^{v} C_{v,o}^{i}\right),\tag{5}$$

is the measured utility (negative of the measured cost) of route r_{ν}^{i} for vehicle ν and α^{ν} , β^{ν} are vehicle-specific constant scalars measuring the sensitivity of traveler ν 's route choice to travel time, which in a sense relates to their value of time. Those parameters can be inferred by the CP through travelers' value of time (Hess, Bierlaire, and Polak, 2004) or past route choice decisions (Nuzzolo and Comi, 2016) etc.

3.2. Correlated Equilibrium (CE)

This subsection first briefly introduces the concept of correlated equilibrium (CE) and then specifies its usage in the proposed routing mechanism. Specifically, we consider an N-player (i.e., vehicles) strategic game (N, A_j , u_j) which is characterized by an action set A_j and utility function u_j for each player j. Let S denote the strategy set given by a trusted CP, let $s \in S$ be a single strategy profile and $s_j \in A_j$ be the action allocated to player j under strategy profile s, i.e., $s = \{s_1, ..., s_N\}$. In a correlated game, a trusted agent assigns actions to every player according to the strategy profile s with a probability distribution $\mathcal{P}(s)$. If no player wants to deviate from the suggested action s_i (deviating from s_i will not receive better expected utility), then a correlated equilibrium (CE) is reached, i.e.,

$$\sum_{s,j} \mathcal{P}(s_{j}, s_{-j}) \left(u_{j}(s_{j}, s_{-j}) - u_{j}(s_{j}', s_{-j}) \right) \ge 0, \ \forall j$$
 (6)

where s'_j is an action of player j different from the suggested action s_j , s_{-j} represents the actions of all other players except j, and u_j is the utility of player j.

In our routing mechanism design, we consider there are two alternatives for each vehicle in their action set A_j , i.e., $A_j = \{a_j^1, a_j^2\}$. Action a_j^1 means that the vehicle v_j follows its individual selfish routing preferences $\{p_o^{v_j,i}\}$, $i=1,...,k^{v_j}$ calculated by Eq. (4), and action a_j^2 means that the vehicle v_j follows the suggested routing preferences $\{p_s^{v_j,i}\}$, $i=1,...,k^{v_j}$ given by the CP. Consequently, under the correlated equilibrium, there will be 2^N possible strategy profile s each associated with probability $\mathcal{P}(s)$. Denote the strategy profile that every vehicle follows the suggested routing preferences (takes the action a_j^2) as s_f , i.e., $s^f = \{a_1^2, a_2^2, ..., a_N^2\}$. Our routing mechanism aims to reach a correlated equilibrium such that $\mathcal{P}(s^f) = 1$ and $\mathcal{P}(s) = 0$, $\forall s \neq s^f$. In other words, every vehicle would be willing to follow the suggested routing preferences. Eq. (6) then becomes

$$0 + 1*\left(u_j\left(a_j^2, a_{-j}^2\right) - u_j\left(a_j^1, a_{-j}^2\right)\right) \ge 0, \ \forall j$$
(6.1)

where a_{-j}^2 represents every vehicle v_j other than v_j takes the action a_j^2 . With this favored equilibrium structure, our routing mechanism aims to design the suggested routing preferences $\{p_s^{v_j,i}\}$, $i=1,...,k^{v_j}$ for each vehicle such that the correlated equilibrium of Eq. (6.1) can be reached, i.e., every rational vehicle would willingly follow the suggested routing preferences (take the action a_i^2).

The routing mechanism design will use CE condition (6.1) to measure individual vehicles' selfish rationality. Namely, we consider that a rational individual will not want to deviate from the routing guidance if it satisfies the CE condition. In other words, the CE condition ensures that no player can be better off by unilaterally deviating from the suggested strategy.

There may be more than one route preference solution satisfying the CE condition (6.1). However, not all of them will lead to a better system-level performance than IR or uoER. Thus, this study is interested in finding a set of optimal suggested routing preferences $\{p_s^{v_j,i}\},\ i=1,...,k^{v_j}$ that maximize the expected system utility in Eq. (7).

System utility:
$$\sum_{s \in S} \sum_{i=1}^{N} \mathcal{P}(s)u_{j}(s_{j}, s_{-j})$$
 (7)

4. Correlated equilibrium Routing Mechanism (CeRM)

Given the research gaps mentioned in the literature review, this study seeks to design a correlated equilibrium routing mechanism (CeRM) that could drive the traffic condition from an inefficient IR to a more systematically optimal one that outperforms existing uoER. By doing that, we consider a traffic scenario where there are a large number of qualified vehicles en route - vehicles equipped with on-board computing and communication devices - trying to make routing decisions in a given short-time period. The CeRM will ensure that every rational vehicle would be better off compared to the now widely adopted IR and would thus follow the scheme voluntarily.

More exactly, there will be an app for individual drivers on their mobile devices. At the beginning of the CeRM navigation service, each participating vehicle provides its OD pairs and personal choice parameters (or relevant information to infer the parameters) and receives the current traffic information (current route travel cost) $C_{v,o}^i$ through the app. Each vehicle's travel information will be sent to the CP by wireless communication technologies under privacy protection algorithms such as Jung et al., 2013). According to the received traffic information, the app for each vehicle ν will calculate their initial routing preference $p_{\nu}^{o,i}$, $i=1,...,k^{\nu}$ (as done in IR by equations (4)-((5)), and then proposed to the CP. The collective information from all vehicles opting in the service is denoted as P_0 $\{p_{i}^{v,i}\}, v=1,...m, i=1,...,k^{v}$. The initial routing preference captures a vehicle's best response to real-time traffic information and is then used by the CP as a reference to design a recommended routing preference that guarantees a better expected utility. Built upon the collected information, the CP will generate the suggested CE route choice preferences $P_s = \{p_s^{v,i}\}, v = 1, ...m, i = 1, ..., k^v$ and then distribute them to each vehicle's app, in which $p_s^{v,i}$, $i=1,...,k^v$ represents the suggested route preference for a driver v. P_s seeks to minimize the system cost (the objective function of Eq. (8.1)) while guarantees every driver would not be better off by deviating from the suggestion (the correlated equilibrium conditions of Eq. (8.2)). Once the app receives the suggested routing preference, it runs in the background and automatically select a route for the vehicle according to the suggested routing preference. The CeRM ensures that travelers will feel satisfied with the suggested routes in general from the long-term cumulative experience of using the app since the expected utility of the suggested preference will be higher than that of the initial preference. The whole process is conducted automatically in the navigation apps/electronic devices, where the drivers only need to provide their OD and personal choice parameters $(\alpha^{\nu}, \beta^{\nu})$ in Eq. (5)) and wait for the app to provide a suggested route.

Note that our solution algorithm designed in Section 5 ensures that the CeRM takes no more than half a minute to generate the optimal CE routing guidance. Considering the traffic condition in such a short time period is not likely to change dramatically, we assume that the initial traffic conditions, i.e., $\{C_{v,o}^i\}$, v=1,...m, $i=1,...,k^v$ won't change during the decision process of the CeRM. If traffic condition changes or travelers change their routes en route for unexpected reasons, they may rejoin the CeRM again as new travelers. For example, the apps on the individual vehicles can periodically reconduct the CeRM to obtain route suggestions whenever they are approaching traffic intersections and have the opportunity to re-route their trips. The calculation will be solved distributedly with the help of vehicles' on-board computation resources, and the suggested route preference will be disseminated to individual vehicles' apps. Each vehicle would then receive a suggested route from the app based on the preferences (probabilities).

4.1. Modeling CeRM

There are a few assumptions we make before introducing the mathematical model for the CeRM:

Assumption 1. Travelers' route choices are formulated as multinomial logit choice models to factor in the uncertainties in their route choice behaviors.

Assumption 2. Every participating driver is rational and would assume all other participants are rational. They will follow the CeRM's recommendations as long as their expected utility can be better off.

Assumption 3. Drivers don't know other drivers' choices.

Assumption 4. Drivers either follow the guidance or stick to their initial route preference calculated by given real-time travel time.

Assumption 5. The link cost function c_l is assumed to be continuously differentiable, strictly increasing, and convex with respect to link flow f_l .

Assumption 1, 2 and 5 are common assumptions used in the transportation field, while Assumptions 3 and 4 capture the properties of the most popular navigation services such as Google or Waze in reality.

The CP suggests individual vehicles the optimal route choice preference by solving the following mathematical programming (MP) problem:

$$\min Z = \sum_{l \in I} f_s^l c_l(f_s^l) \tag{8.1}$$

s.t

$$\sum_{i=1}^{k_{v}} p_{s}^{v,i} \left(-C_{v}^{i}(\mathbf{P}_{s}) - \frac{1}{\beta_{v}} \ln(p_{s}^{v,i}) \right) \ge \sum_{i=1}^{k_{v}} p_{o}^{v,i} \left(-C_{v}^{i}(\mathbf{P}_{o}^{v}) - \frac{1}{\beta_{v}} \ln(p_{o}^{v,i}) \right), \ \forall v = 1, ..., m$$

$$(8.2)$$

$$\sum_{i=1}^{k_{\nu}} p_s^{\nu,i} = 1, \ \forall \nu = 1, ..., m$$
 (8.3)

$$p_{\star}^{v,i} > \epsilon, \ \forall v = 1, ..., m, \ \forall \ i = 1, ..., k^v$$
 (8.4)

$$f_{s}^{l} = \sum_{v=1}^{m} \sum_{i=1}^{k^{v}} p_{s}^{v,i} \delta_{v,i}^{L}, \ \forall l \in L$$
 (8.5)

Where, $P_o^v = \{p_s^{v_1,i_1}, \dots, p_s^{v-1,i_{k^v-1}}, p_o^{v,i_1}, \dots, p_s^{v,i_{k^v}}, p_s^{v+1,i_1}, \dots, p_s^{v_m,i_{k^vm}}\}$ is the set of route choice preferences in which only vehicle v sticks to its initial preferences $p_o^{v,i}$ and all others follow the CeRM guidance. Specifically, P_o^v is a vector containing the routing preferences of all vehicles, in which vehicle v's routing preference is $\{p_o^{v,i_1}, \dots, p_o^{v,i_{k_v}}\}$, and all other vehicles $v' \neq v$ are $\{p_s^{v',i_1}, \dots, p_s^{v',i_{k_v'}}\}$. Accordingly, the expected link flow for vehicle j on link l if it deviates from the suggested routing preference can be calculated by $f_{v_j}^l = \sum_{v=1}^{m \setminus v_j} \sum_{i=1}^{k^v} p_o^{v,i} \delta_{v,i}^l + \sum_{i=1}^{k^v} p_o^{v,i} \delta_{v,i}^l$.

The MP aims to find an optimal solution that maximizes system utility (minimizes total system cost) (8.1) while satisfying the correlated equilibrium condition (8.2) and other related feasibility constraints. Note that f_s^l is the expected flow on link l if everyone follows the CeRM routing guidance P_s . Thus, the objective function (8.1) here is the expected total system travel time incurred by all vehicles in the network. The objective function can also incorporate other performance measurements such as emissions. It won't affect the applicability of our model and the solution approach as long as its gradient satisfies the Lipschitz continuous condition. The left-hand side of Equation (8.2) is the driver's expected utility if they follow the guidance (i.e., $u_v(a_j^2, a_{-j}^2)$ in Equation (6.1)), and the right-hand side is the expected utility if he unilaterally deviates from the guidance (sticks to their original routing preference P_o^v , i.e., $u_v(a_j^1, a_{-j}^2)$ in Equation (6.1)). We refer to constraint (8.2) as the rationality constraint, since it represents the decision process a rational driver would consider Assumption 3 and 4. Below gives a further explanation of the constraints.

It has been well-known that under discrete behavior choice models, the perceived utility $U_{v,i}$ of a route i for vehicle v considers not only the exact measured travel time $V_{v,i}$, but also a random term ε that represents the influence of unobserved attributes or measurement errors (such as travel time uncertainty) (Sheffi, 1985), i.e., $U_{v,i} = V_{v,i} + \varepsilon$. Under the commonly adopted multinomial logit choice model, the error term ε follows an i.i.d Gumbel distribution. The welfare/consumer surplus (Small and Rosen, 1981) (also known as uncertainties (Yang, 1999)) an individual vehicle v receives if it chooses a particular route i among other candidate routes could then be expressed as $-\frac{1}{\beta_v}p^{v,i}\ln(p^{v,i})$ (Small and Rosen, 1981; Yang, 1999). Then, the utility (net economic benefit) of an individual vehicle could be expressed as the welfare it receives minus the transportation cost it experiences (Yang, 1999), i.e., $\left(-\frac{1}{\beta_v}p^{v,i}\ln(p^{v,i}) - p^{v,i}C_v^i(P)\right)$. It is worth noting that under the CeRM, the suggested routing preference p_s^v of each individual vehicle are calculated from the MP rather than determined by logit choice model. But as a rational driver possesses consistent behavior patterns throughout a decision-making process to determine whether to follow the independent routing preference p_o^v or the suggested routing preference p_s^v , it is reasonable to use the consistent measurement to measure the utility of the decision from an individual driver's view. Namely, a

decision-making process to determine whether to follow the independent routing preference p_o^v or the suggested routing preference p_s^v , it is reasonable to use the consistent measurement to measure the utility of the decision from an individual driver's view. Namely, a rational driver would choose the routing decision with the largest expected utility. To ensure compliance with the equilibrium routing guidance, the rationality constraints (8.2) guarantee that each driver would not be better off (receive more expected utility) if they choose not to follow the proposed guidance. In other words, if constraints (8.2) are satisfied, each driver would have no incentive to deviate from the suggested routing guidance. To implement the CeRM in practice, the expected utility can be converted to a customer-friendly (such as monetary) value to sustain travelers' compliance. How to conduct this conversion reliably itself is a research problem and has obtained much interest in literature (Mongin, 1998). Here, we only give a simple example to illustrate the idea. The expected utility in this study consists of two parts respectively representing the expected travel time ($\sum_{i=1}^{k_v} p_s^{v,i} C_{i}^i(P)$) and travel time related uncertainty ($\frac{1}{l_p}$, $\sum_{i=1}^{k_v} p_s^{v,i} \ln(p^{v,i})$) (Yang, 1999). The expected travel time can be converted to monetary value by the value of uncertainty (Van Amelsfort and Bliemer, 2005). Putting together we can get a monetary value for the expected utility.

Constraints (8.3) – (8.4) ensure the conservation and positiveness of probability variables. It's worth pointing out that the route preference (probability) under the logit choice model is strictly positive. Namely, each route's probability could not be 0 because of uncertainties and user heterogeneities. To align the same route choice behavior pattern of a rational driver, constraints (8.4) ensure that the decision variables of route choice preference are positive. Here, we set ε as a sufficiently small positive constant, e.g., $\varepsilon = 1 \times 10^{-6}$. According to the theory of bounded rationalities (Simon, 1955; van Essen et al., 2016), a rational driver cannot sense the travel time difference within a certain threshold. Thus, the introduction of ε to constraints (8.4) would not cause any noticeable difference to the routing decision of an individual driver in practice, but will affect our solution algorithm design and convergence proof under random communication failures. We will discuss these technical issues in later sections. Constraints (8.5) are flow conservation constraints.

From a mathematical point of view, the MP of (8.1) – (8.5) has a convex objective function but nonconvex constraint sets, and the detailed proof is shown in Appendix A. Moreover, the MP is always feasible. When no routing guidance is given to individual vehicles, i.e., $P_s = P_o$, all the constraints are satisfied, which means that there always exists a feasible solution for our problem. For simplicity issue, we reform the rationality constraint as:

$$r_{v}(\mathbf{P}_{s}) = \sum_{i=1}^{k_{v}} p_{s}^{v,i} \left(C_{v}^{i}(\mathbf{P}_{s}) + \frac{1}{\beta_{v}} \ln(p_{s}^{v,i}) \right) - \sum_{i=1}^{k_{v}} p_{o}^{v,i} \left(C_{v}^{i}(\mathbf{P}_{o}^{v}) + \frac{1}{\beta_{v}} \ln(p_{o}^{v,i}) \right) \le 0, \ \forall v = 1, ..., m$$

$$(9)$$

5. Distributed and Robust Solution Algorithm

The CeRM seeks to provide online routing guidance for every participating vehicle to mitigate traffic congestion. It requires us to solve the large-scale, highly coupled, and nonlinear nonconvex MP in (8.1) – (8.5) promptly (i.e., less than 30 seconds) since it is not likely that a driver en route would wait several minutes or even longer to get the route guidance. Even though there exist many methods to cope with nonconvex optimization problems, such as interior-point methods (Boggs and Tolle, 1995), SQP (sequential quadratic programming) (Boggs and Tolle, 1995), and problem-specific heuristic algorithms (Ma, Smith, and Zhou, 2016), etc., state of art shows that none of them could satisfy the computation needs for such online service involving a large scale of vehicles in a large transportation network (i.e., a large number of decision variables). On the other hand, thanks to recent developments in vehicular on-board computing devices and wireless communication technologies, distributed computation is becoming a possible solution to be implemented in practice. However, distributed computation often requires extensive data exchanges between different computation agents. Implementing distributed computation in this application will rely on the wireless communication stability between CP and the vehicles. This concern indicates that our algorithm design should consider the effect of communication failures since unstable wireless communication may jeopardize the computation performance.

Motivated by this view, this study develops a distributed and robust solution algorithm, i.e., distributed Augmented Lagrangian (D-AL), to solve the proposed MP for the CeRM problem by taking advantage of the problem's unique structure features. Mainly, the D-AL will efficiently solve the problem by distributing a large portion of the computation loads to individual CVs while maintaining robustness against connection loss and communication failures, which frequently appear in real-world scenarios. Fig. 1 illustrates the framework of the D-AL implemented between the CP and individual vehicles. Specifically, it includes the four essential procedures.

Step (i): Individual vehicles first locally evaluate traffic conditions and propose their routing preferences to the CP;

Step (ii): Upon receiving the information, the CP forms the MP for the CeRM problem, transforms it into a separable problem (MP - S), and then separated into individual problems (MP - I) and dispatch to each vehicle;

Step (iii): Each vehicle iteratively calculates the assigned computation tasks and proposes the result to the CP. The CP synchronizes individuals' responses and updates the solution until the MP-S converges;

Step (iv): If the outcome of Step (iii) does not satisfy the convergence criteria of the MP for the CeRM model, the MP - S is updated and the algorithm returns to step (ii).

Note that the communications between the individual vehicles and the CP in Step (iii) are not always stable. Probably, some vehicles may temporarily lose connections and fail to respond to the CP in time, which are represented as the dashed line in Fig. 1. The proposed D-AL is robust to such unstable communications and is guaranteed to converge to a local solution to the MP of our CeRM problem. The subsections below introduce the technical details for developing such a solution algorithm, including model transformation, distribution scheme, and a customized projection algorithm, while the robustness of the D-AL is discussed following that.

For simplicity issues, we denote the solution (routing guidance) of our problem $P_s = \{p_s^{v,i}\} = \{x^{v,i}\} = X \in \mathbb{R}^{\sum_{v} k^v}$ hereafter.

5.1. Distributed Augmented Lagrangian (D-AL) algorithm

5.1.1. The Augmented Lagrangian Transformation

To develop the D-AL, we first notice that the MP's constraint set (8.2) - (8.5) presents a unique feature. It involves complicated nonconvex and highly coupled rationality constraints (8.2) and a relatively simple and separable ε -probability simplex constraint set (8.3) - (8.4) regarding each vehicle's route choice decision variables (preference). Invoked by these features, we consider transforming the MP for the CeRM problem into the Augmented Lagrangian form (10) by changing the inequality constraints (9) (an equivalent transformation of rationality constraints (8.2)) into equality constraints and penalizing them into the objective function (8.1).

$$\mathscr{L}(X, \lambda_{K}, c_{K}) = \underbrace{\sum_{L=1}^{n} f_{s}^{L} c_{L}(f_{s}^{L})}_{Z} + \frac{1}{2c_{K}} \sum_{\nu=1}^{m} (\max^{2} \{0, \lambda_{K}^{\nu} + c_{K} r_{\nu}(X)\} - \lambda_{K}^{\nu}^{2}), \tag{10}$$

where $\lambda_K = \{\lambda_K^{\nu}\}$, $\nu = 1, ..., m$ is the set of Lagrangian multipliers, and c is the penalty parameter. Then we have the first transformations of the MP for the CeRM problem given below.

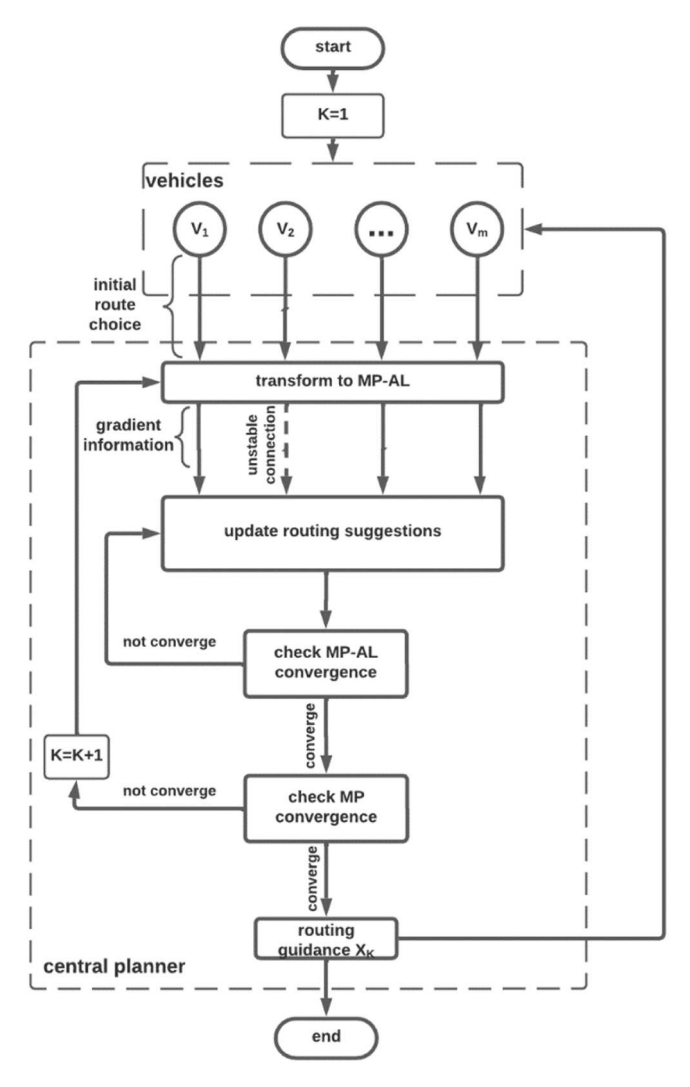


Fig. 1. The flow chart of the D-AL solution algorithm.

$$MP - AL : \min_{X} \mathcal{L}(X, \lambda, c)$$

$$s.t. (8.3) - (8.5)$$
(11)

The merits of this transformation lie in eliminating the complex constraints (8.2) in the MP and transforming them into more manageable sub-problems. Accordingly, existing studies (Bertsekas, 1997) show that by iteratively solving and updating the transformed problem in (11) and associated parameters by the Augmented Lagrangian method (AL), we can find a local solution of the MP developed for the CeRM. Below in Table 1 we first briefly introduce the procedure of the AL algorithm to update the Lagrangian multipliers λ_K and penalty parameter c_K with the given solution of (11):

Where $\mathcal{J} = \max_{v \in V} r_v(X)$ is the maximum violation of all rationality constraints, $\gamma_c > 1$ is a constant scalar for updating c_K , γ_m is a positive constant to compare the change in constraint violations, and X_K is the solution of (11) corresponding to (λ_K, c_K) . The AL stops

Table 1 Parameter updating scheme.

1:	if $\mathcal{Y}_{K+1} \leq \gamma_m \mathcal{Y}_K$ (rationality constraint violation has been decreased):
2:	$set c_{K+1}=c_K;$
3:	else:
4:	$\operatorname{set} c_{K+1} = \gamma_c c_K;$
5:	end if;
6:	for $v \in V$:
7:	$\operatorname{set} \lambda_{K+1}^{\nu} = \max\{0, \lambda_{K+1}^{\nu} + c_K r_{\nu}(X_{K+1})\};$

until the convergence criterion of the MP for the CeRM problem is satisfied. The updating scheme of the Lagrangian multipliers takes the merit of Augmented Lagrangian algorithms and the updating scheme of the penalty parameter c_K has shown to be efficient for our problem in numerical experiments.

On the other hand, with each given parameters (λ, c) , the AL algorithm solves the transformed problem in (11) by iteratively updating the solution using the gradient projection method as follows.

$$X_{k+1} = \left[X_k - \alpha^k \nabla \mathscr{L} \right]^{\mathscr{V}},\tag{12}$$

where $[\cdot]^{\mathscr{H}}$ stands for the projection onto the constraint set (8.3) – (8.4) denoted by \mathscr{H} and α^k is the step size. Note that we use upper case K to denote each iteration of updating Lagrangian multipliers and penalty parameter ($\lambda_K c_K$), and lower case k to denote the iteration of updating X_k for a given transformed problem (11). However, the standard gradient projection method along with the AL algorithm is not efficient enough to satisfy the computation need of our online navigation service. This study further develops a distribution scheme and a customized ε -probability simplex projection algorithm to expedite the computation of the solution algorithm.

5.1.2. Distribution scheme

It is noticed that the link-based objective function (8.1) (the first item Z in (10)) is not user separable, but the second item in (10) and the constraint set (8.3) – (8.4) are. Thus, to accommodate a distribution scheme, we transform the objective function Z into the equivalent path-based and user separable form Z_{ij} :

$$Z_{u} = \sum_{\nu=1}^{m} \sum_{i=1}^{k_{\nu}} p_{s}^{\nu,i} C_{\nu}^{i}(\mathbf{P}_{s})$$
(13)

After this second transformation, the objective function (10) can be rewritten as the summation of individuals' augmented objective functions in (14) (i.e., MP - AL of (11) is then transformed to MP - S of (14)), which could then be separated among individual vehicles.

$$MP - S: \min_{\mathbf{X}} L(\mathbf{X}, \lambda, c) = Z_u + \frac{1}{2c} \sum_{\nu=1}^{m} \left(\max^2 \{0, \lambda^{\nu} + cr_{\nu}(\mathbf{X})\} - \lambda^{\nu 2} \right) = \sum_{\nu=1}^{m} f_{\nu}$$

$$s.t. (8.3) - (8.5)$$
(14)

Where $f_{\nu} = \sum_{i=1}^{k_{\nu}} p_{s}^{\nu,i} C_{\nu}^{i}(P_{s}) + \frac{1}{2c} \sum_{\nu=1}^{m} (\max^{2}\{0, \lambda^{\nu} + cr_{\nu}(X)\} - \lambda^{\nu 2})$ is the individual vehicle's augmented objective function. The first part of f_{ν} is the expected travel cost of vehicle ν and the second part is related to the violation of vehicle ν 's rationality. From the individual's perspective, a vehicle ν only cares about its own augmented objective f_{ν} , and tries to minimize it subject to constraints (8.3) – (8.5). We refer to the following model for each vehicle ν as the individual problem (MP - I).

$$MP - I : \underset{X^{v}}{minf_{v}}(X^{v}, \lambda, c) = \sum_{i=1}^{k_{v}} p_{s}^{v,i} C_{v}^{i}(P_{s}) + \frac{1}{2c} \left(\max^{2} \{0, \lambda^{v} + cr_{v}(X^{v})\} - \lambda^{v2} \right)$$

$$s.t. (8.3) - (8.5)$$
(15)

Note that an MP-I is a separation of MP-S regarding vehicles, not the decision variables. Namely, each MP-I holds the same decision variables as the MP-S. It can be seen as an individual vehicle ν trying to design routing preferences for all vehicles that minimize its own augmented objective. An MP-I can also be solved using the gradient projection method by iteratively performing the updating process shown in (16):

$$\boldsymbol{X}_{k+1}^{v} = \left[\boldsymbol{X}_{k}^{v} - \alpha^{k} \nabla f_{v}\right]^{\mathscr{H}}$$
 (16)

Where, $X^{\nu} \in \mathbb{R}^{\sum_{\nu} k^{\nu}}$ is the solution of vehicle ν 's MP-I. A solution X^{ν} from vehicle ν can be seen as the solution mostly favorable to vehicle ν 's interest. However, for two vehicles, most likely we will have $X^{\nu} \neq X^{\nu}$. Consequently, X^{ν} is not in accordance with the overall objective in (14). To balance individuals' will and produce a consensus solution that converges to the P-S, we design a customized distribution scheme (c-DS) that only requires (the app of) the individual to calculate and propose their interest-related gradients $\nabla f_{\nu} = \left\{\frac{\partial f_{\nu}}{\partial p_{i}^{\nu_{1},1_{1}}}, \ldots, \frac{\partial f_{\nu}}{\partial p_{i}^{\nu_{m},k_{vm}}}\right\}$. Note that the app on the individual vehicle will automatically run in the background to conduct related computations, just like most navigation apps such as Google maps will use local computation resources from their user's devices. By synchronizing individuals' gradients, the CP can obtain $\nabla \mathscr{L} = \sum_{\nu=1}^{m} \nabla g_{\nu}$, and then perform the update through (17) to solve the MP-S of (14).

$$\boldsymbol{X}_{k+1} = \left[\boldsymbol{X}_k - \alpha^k \sum_{\nu=1}^m \nabla f_\nu\right]^{\mathscr{H}} \tag{17}$$

Here, the step size α^k is determined by a centralized line search along the projection arc (Bertsekas, 1997). Clearly, $\sum_{\nu=1}^{m} \nabla f_{\nu} = \nabla \mathcal{L}$ and the solution updating process (17) is equivalent to performing the gradient projection algorithm (12) on the MP - AL (11), but

using a distributed way to conduct this computation.

This study also noticed another more general and straightforward way to distribute the calculation load of $\nabla \mathscr{L}$ in (12) by letting each vehicle compute the partial derivatives related to their own decision variables. We label this naive approach as n-DS: vehicle ν computes $\frac{\partial \mathscr{L}}{\partial p_i^{\nu}}$, $i=1,...,k_{\nu}$. However, there are two drawbacks in n-DS. First, unlike in c-DS, individuals have no direct interest in the computation task under n-DS, making them less willing to contribute their computing power and propose the needed information. Second, the naive approach n-DS is less efficient than our problem-specific c-DS regarding the computation workload. We prove this merit in Theorem 1 below.

Theorem 1. Assume there are m vehicles each with k possible candidate routes, then each vehicle undertakes $\frac{1-\frac{1}{m}}{k+1}$ less workload in c-DS than in n-DS.

Proof: see Appendix B.

It is worth noting that each vehicle usually faces 2 to 4 possible routes. Then the c-DS developed in this study can reduce the computation load by nearly 20% to 33%, which is quite considerable in practice given that the main computation burden of the D-AL lies in this part.

5.1.3. Projection onto the ε -probability simplex

It should be noted that the updating process (17) involves a projection process $[\cdot]^{\mathscr{H}}$, which is not easy to perform in general procedures. It usually involves solving a quite computationally costly optimization problem: $\min_{x \in \mathscr{H}} \|x - y\|$. However, after conducting the Augmented Lagrangian transformation and further transforming the problem to MP - S in (14), the remaining constraints are of ε -probability simplex form for each vehicle. Several studies, i.e., (Chen and Ye, 2011; Wang and Carreira-Perpinán, 2013) have developed projection algorithms with the probability simplex ($x_i \ge 0$, $\sum_i x_i = 1$). To be noted, our study works on the projection onto

the ϵ -probability simplex space. Thus, we cannot directly use their algorithms. This subsection thus develops a ϵ -simplex projection algorithm that could conduct the projection efficiently to the ϵ -probability simplex space without solving the extra optimization problem. We first give the projection algorithm in Table 2 and then prove its correctness.

The main complexity of the algorithm lies in sorting the elements of Y into descending order, which has a worst-case time complexity of $O(n\log n)$ (Cormen et al., 2009). Theorem 2 below proves the algorithm correctly projects a vector into the ε -probability simplex space.

Theorem 2. the ε-Simplex Projection algorithm returns a vector X that satisfies $X = \arg\min_{X \in \mathcal{X}} ||X - Y||^2$, where \mathcal{X} is the ε-probability simplex space.

Proof: see Appendix C.

With the help of our customized distribution scheme (sec 5.1.2) and ε -Simplex Projection algorithm, a complete description of Step (iii) in D-AL can then be given as follows: After an MP-S is formed in Step (ii), the CP distributes individual-specific objective functions along with the current step solution to each vehicle. Upon receiving the information, individual vehicles calculate the gradients related to their own functions and propose them to the CP. The CP then aggregates all the information and performs process (17) to update a new solution. This process keeps iterating until the MP-S is converged. The solution updating process of (17) takes the merit of the gradient projection algorithm and is guaranteed to converge to a local solution of MP-S (Bertsekas, 1997). Given the solution accuracy requirement, the computation time complexity for D-AL to solve the CeRM problem has a quadratic relation with the number of vehicles and the candidate paths for each vehicle. The detailed proof for the computation time complexity analysis can be found in Lemma 14 in Appendix G.

To this end, combining Sections 5.1.1 - 5.1.3, we provide the steps of the D-AL in Table 3.

The D-AL algorithm developed here heavily relies on the distributed computation of the gradient information, i.e., $\sum_{v=1}^{m} \nabla f_v$ in (17). Specifically, when the computation results aggregated from individual vehicles are exactly the gradient of the MP-S ($\nabla \mathscr{L}$), the solving process (17) of MP-S takes the merits of the gradient projection methods and guarantees to converge (Bertsekas, 1997). Then, as MP-S is iteratively updated according to (11) and the Parameter updating scheme, the convergence of the D-AL resembles that of the Augmented Lagrangian algorithm (see sec 5.1.1), which has been proved in literature to converge to a local solution (Bertsekas, 1997). In other words, the convergence of D-AL is guaranteed when every vehicle is well-connected throughout the navigation process. However, in real-world scenarios, communications between vehicles and the CP may not always be stable. There are times when one or

Table 2 ε-Simplex Projection Algorithm.

	3	0	
1:			input $Y=(y_1,,y_n)\in\mathbb{R}^n;$
2:			sort <i>Y</i> in descending order such that $y_{(1)} \ge y_{(2)} \ge \ge y_{(n)}$;
3:			find the largest index $k \in [1, n]$, such that
			$egin{aligned} oldsymbol{y}_{(k)} - rac{\sum_{i=1}^k oldsymbol{y}_{(i)} + (n-k)\epsilon - 1}{k} > \epsilon \end{aligned}$
4:			$\operatorname{set} \lambda = \frac{\sum_{i=1}^k y_{(i)} + (n-k)\epsilon - 1}{k}$
5:			return $x_i = \max \{y_i - \lambda, \varepsilon\}, i = 1,, n.$

Table 3 D-AL solution algorithm.

1:	Initialization : initial route choice probabilities p_{ν}^{i} , $i=1,,k_{\nu}$, $\nu=1,,m$, Lagrangian multipliers λ_{1} and penalty parameter c_{1} ;
2:	For $K = 1, 2,, :$
3:	If the convergence criterion of the MP for the CeRM problem is satisfied:
4:	break;
5:	Else:
6:	transform to / update $(\lambda_K c_K)$ for the $MP-S$ according to Eq. (11), (14) and the Parameter updating scheme;
7:	For $k = 1, 2,,$:
8:	If the convergence criterion of the $MP - S$ is satisfied:
9:	break;
10:	Else:
11:	distribute computation task ∇f_{v} to each vehicle v ;
12:	collects the result from each vehicle and update the route choice probabilities according to Eq. (17) with the help of Algorithm 1;
13:	End
14:	End

multiple participating vehicles temporally lose connections due to poor network environment or on-board equipment malfunctioning. Then, two critical questions need to be answered to demonstrate the practicability of the D-AL algorithm in this online application: (1) will the D-AL converge under unstable connections (communication failures/connection loss); (2) how fast the D-AL will converge under unstable connections. The following subsection will theoretically discuss the D-AL's convergence, robustness, and resilience against random communication failures.

5.2. Robustness and Resilience against Random Communication Failures

This section analyzes the convergence properties under more realistic scenarios where connections between individual vehicles and the CP are not perfectly stable. We provide rigorous proofs for the convergence and convergence rate of the D-AL algorithm under communication failures. Having recognized that the commutation failure will jeopardize the convergence efficiency of the D-AL, we further give a distribution scheme that could expedite the convergence. Throughout this section, we assume that a random proportion of the vehicles would drop out of the connection during the navigation process of the CeRM but would eventually reconnect at some point (still participating in the navigation). Specifically, during each round of the communication (i.e., a single update of (17)), every vehicle might lose connection and fail to respond to the D-AL in time with probability q>0 and might stay well connected with probability 1-q. These probabilities are independent between vehicles and between each round of communication.

Under **perfect connection scenarios**, the gradient information used in each update (17) can then be expressed as $\nabla \mathscr{L} = \sum_{i=1}^{m} \nabla f_{V_i}$ $= \nabla \mathscr{F}^T 1_m$, where $\nabla \mathscr{F} = (\nabla f_{V_1}, ..., \nabla f_{V_m})^T$ is the column vector of ∇f_{V_i} , i = 1, ..., m, and 1_m is the all-ones column vector of size $m \times 1$. Denote $\mathbf{B} = (b_1, ..., b_m)^T$, where b_i , i = 1, ..., m indicates whether vehicle v_i is connected, i.e., b_i is a Bernoulli random variable, which takes value 1 with probability (1 - q) when vehicle v_i is well-connected and 0 otherwise with probability q. Under **imperfect connection scenarios**, the CP receives partial gradient information $(b_1 \nabla f_1, ..., b_m \nabla f_m)$ from the individual vehicles and uses the approximated gradient \mathbf{G} defined in (18) as an approximation of the true gradient $\nabla \mathscr{L}$, where s is the number of disconnected vehicles and $\frac{m}{m-s}$ is a weighted sum coefficient which turns the partial information the CP received from well-connected vehicles to approximate the overall gradient information of all vehicles.

$$G = \frac{m}{m-s} \nabla \mathcal{F}^T \mathbf{B} \tag{18}$$

Then, the update of (17) becomes

$$\boldsymbol{X}_{k+1} = \left[\boldsymbol{X}_k - \alpha^k \boldsymbol{G}_k\right]^{\mathscr{K}}, \text{ where,} \boldsymbol{G}_k = \frac{m}{m-s} \nabla \mathscr{F} (\boldsymbol{X}_k)^T \boldsymbol{B}$$
(19)

Clearly, $s = m - \sum_{i=1}^{m} b_i$ and the exact value of s during each update is only known to the CP after the communication process in an updating iteration ends. Note that existing literature (Bertsekas, 1997; Iusem, 2003) shows that the convergence properties of the projected gradient descent method are essentially the same as the gradient descent method in the unconstrained case. Therefore, in the following context, we will omit the projection operator $[\cdot]^{\mathscr{H}}$ and analyze the convergence properties based on the unconstrained gradient descent update of the form (20):

$$X_{k+1} = X_k - \alpha^k G_k \tag{20}$$

5.2.1. Convergence of the D-AL under random communication failures

The key step to prove the convergence of the D-AL is to confirm that each transformed problem (14), i.e., the MP-S, could converge under the updating process of (20). As discussed in sections 5.1.1 and 5.1.2, if the MP-S converges and is updated according to the parameter updating scheme, then the D-AL performs as an Augmented Lagrangian algorithm and is guaranteed to converge to a first-order optimality solution of the original problem (Bertsekas, 1997). In this sub-section, we prove the convergence of the D-AL to the MP of our CeRM problem by showing that the MP-S will converge under random communication failures. We apply a general

theorem regarding the convergence of gradient methods with stochastic errors. To be self-contained, we provide the existing theorem below

Theorem 3. (Bertsekas and Tsitsiklis, 2000; Bottou, Curtis, and Nocedal, 2018); For the problem

$$ming(x)$$
 subject to $x \in \mathcal{R}^n$,

such that for some constant ϕ we have $\|\nabla g(x) - \nabla g(\bar{x})\| \le \zeta \|x - \bar{x}\| \ \forall x, \ \bar{x} \in \mathscr{R}^n$.

Let x_k be a sequence generated by the method

$$x_{k+1} = x_k - \alpha_k (d_k + \omega_k),$$

where α_k is a deterministic positive step size, d_k is a descent direction, and ω_k is a random noise term. If the following assumptions hold:

(a) There exist positive scalars c_1 and c_2 such that

$$c_1 \| \nabla g(x_k) \|^2 < \nabla g(x_k)^T d_k, \| d_k \| < c_2(1 + \| \nabla g(x_k) \|) \forall k$$

(b) For a positive scaler c_3 , we have

$$E(d_k + \omega_k) = c_3 d_k \ \forall k$$

(c) For a positive constant A, we have

$$E(\|\omega_k\|^2) < A(1+\|\nabla g(x_k)\|^2) \ \forall k$$

(d) We have

$$\sum_{k=0}^{\infty} lpha_k = \infty, \,\, \sum_{k=0}^{\infty} lpha_k^2 < \infty.$$

Then, either $g(x_k) \to -\infty$ or else $g(x_k)$ converges to a finite value and $\lim_{k \to \infty} \nabla g(x_k) = 0$. Furthermore, every limit point of x_k is a stationary point of g.

Remark 4. The original Theorem in (Bertsekas and Tsitsiklis, 2000) requires in assumption (b) that $E(\omega_k) = 0$, which means that the descent direction with error is an unbiased estimator of the true descent direction, i.e., $E(d_k + \omega_k) = d_k$. Further studies have extended the requirement such that the descent direction with error could be an unbiased estimator of the true descent direction up to a constant factor (Bottou, Curtis, and Nocedal, 2018), i.e., for a positive constant c_3 , $E(d_k + \omega_k) = c_3 d_k$, which can be easily transformed to the original requirement by multiplying the step size with a constant factor $\frac{1}{c_3}$ (Raviv et al., 2020).

We next translate the items in our problem to that in Theorem 3 so that we can apply this theorem to prove the convergence of our algorithm. Specifically, the objective function $\mathcal{L}(X)$ corresponds to g(x), the gradient of the objective function, $\nabla \mathcal{L}$, corresponds to the true descent direction d_k , and then the approximated gradient G corresponds to the descent direction with error $d_k + w_k$ in Theorem 3 respectively. To guarantee the convergence of the D-AL using gradient methods with stochastic errors, Theorem 3 requires four conditions: 1) $\nabla \mathcal{L}$ is ζ Lipschitz continuous; 2) $\nabla \mathcal{L}$ satisfies assumption (a); 3) G is an unbiased estimator of the true descent direction up to a constant factor (assumption (b)); 4) the random error ω_k has bounded variance relative to the gradient (assumption (c)). Accordingly, our procedures to prove that the problem structure of the MP - S and the solution updating process (20) satisfies the assumptions of Theorem 3 rely on Lemma 5 – 8: (i) Lemma 5 shows that the approximated gradient G is an unbiased estimator of the true gradient ∇L up to a constant factor. (ii) Lemma 6 shows that the gradient ∇L is bounded and ζ Lipschitz continuous. (iii) Lemma 7 and Lemma 8 show that the approximation error $(G - \nabla \mathcal{L})$ has bounded variance relative to $\nabla \mathcal{L}$. Last, Theorem 9 concludes the convergence of the D-AL using Theorem 3 and Lemma 5 – 8. The following context provides the technical details.

Lemma 5. The approximated gradient G in (18) is an unbiased estimator of the true gradient $\nabla \mathcal{L}$ up to a constant factor σ , i.e.,

$$E(G) = \sigma \nabla \mathscr{L},$$

where $\sigma = 1 - q^m$.

Proof: See Appendix D.

Lemma 6. The gradient of the objective function \mathcal{L} of the MP - S (14) is bounded and ζ Lipschitz, i.e., there exists positive constants

 $u_{\mathcal{L}}$ and ζ , such that

$$\|\nabla \mathcal{L}(\mathbf{X})\| \leq u_{\mathcal{L}}$$

$$\parallel \nabla \mathcal{L}(X) - \nabla \mathcal{L}(\bar{X}) \parallel \leq \zeta X - \bar{X} \parallel$$

Proof: See Appendix D.

Lemma 7. Variance of the gradient approximation error, measured by $\phi_{D-AL} = E(\|\mathbf{G} - \nabla \mathcal{L}\|^2)$, is bounded relative to $\nabla \mathcal{F} = (\nabla f_{\nu_1}, ..., \nabla f_{\nu_m})^T$, i.e.,

$$\phi_{D-AL} = E(\parallel \mathbf{G} - \nabla \mathcal{L} \parallel^2) \leq \frac{mq}{1-q} \parallel \nabla \mathcal{F} \parallel^2$$

Proof: See Appendix D.

Lemma 7 indicates that the upper bound of the variance of the approximation error would increase as the probability of the communication failures increases, which in turn affects the convergence rate of the solution algorithm, as will be discussed in the next sub-section.

Lemma 8. $\nabla \mathscr{F} = (\nabla f_{\nu_1}, ..., \nabla f_{\nu_m})^T$, where f_{ν_i} is the objective function of MP - I (15) for vehicle ν_i , is bounded, i.e., $\|\nabla \mathscr{F}\| \le u_f$, where u_f is a positive constant.

Proof: See Appendix D.

Lemma 8 combined with the result in Lemma 6 that $\|\nabla \mathcal{L}\| \le u_{\mathcal{L}}$ and the result in Lemma 7 that $E(\|G - \nabla \mathcal{L}\|^2) \le \frac{mq}{1-q} \|\nabla \mathcal{F}\|^2$, it's easy to see that by letting $A \ge \frac{mqu_T^2}{(1-q)(1+u_T^2)}$, we will have

$$E(\parallel \mathbf{G} - \nabla \mathcal{L} \parallel^2) \leq \frac{mq}{1 - q} u_f^2 \leq A(1 + \parallel \nabla \mathcal{L} \parallel^2)$$

Theorem 9. The D-AL guarantees to converge to a first-order optimality solution of the MP - S of (14) under random communication failures.

Proof: See Appendix D.

5.2.2. Convergence Rate of the D-AL under Random Communication Failures

Recall that the CeRM is developed for online routing guidance. Thus, it is not sufficient to only guarantee the convergence of the D-AL algorithm under random communication failures. To ensure the applicability of the D-AL, we also want to know how fast the D-AL could converge and how the communication failures would affect the convergence rate. In this subsection, we theoretically demonstrate the convergence rate of the D-AL algorithm and then discuss its relationship with the disconnection probability q. We address these critical theoretical questions with significant application impact by proving Theorem 10 and Corollary 11.

Note that the overall computation time T for our algorithm to converge equals the sum of the computation time t_k to conduct a single iteration of (20), i.e., $T = \sum_{k=1}^{N} t_k$, where N is the number of iterations the algorithm takes to converge. As t_k is independent of N, the number of iterations is then an important indicator of the convergence rate. Naturally, the greater number of iterations leads to a longer overall computation time and thus a slower convergence rate. While a few studies have worked on the convergence rate of general stochastic gradient methods, they cannot be directly applied to our study. Some of them have assumptions on convexity (e.g. (Nemirovski et al., 2009)) that our problem structure does not satisfy, and others adopt solution updating schemes that are different from (20) of our algorithm. For example, the solution algorithm in (Reddi et al., 2016) uniformly and randomly takes partial elements from the true gradient to form the approximated gradient. Interested readers can refer to (Bottou, Curtis, and Nocedal, 2018) for a comprehensive review. The following Theorem 10 demonstrates how the number of iterations in our algorithm is affected by the approximation error, which is partially adapted from (Ghadimi and Lan, 2013) that discusses the convergence properties of general stochastic first- and zeroth-order methods.

Theorem 10. The number of iterations of the D-AL algorithm with the communication failures takes to reach a ε-accurate solution for the MP-S (14) (i.e., $E(\|\nabla \mathcal{L}\|^2) \le \varepsilon$) is of $O\left(\frac{\phi^2}{\varepsilon^2}\right)$, where $\phi=E(\|G-\nabla \mathcal{L}\|^2)$ measures the variance of the approximation error.

Proof: See Appendix E.

Combining Theorem 10 with Lemma 7 and Lemma 8, we could get the relationship between the convergence rate and the disconnection probability q:

Corollary 11. The number of iterations the D-AL algorithm with communication failures takes to reach a ε -accurate solution (i.e., $E \parallel \nabla \mathscr{L} \parallel^2 \leq \varepsilon$) is of $O\left(\frac{1}{(1-q)^2\varepsilon^2}\right)$, where q is the disconnection probability of individual vehicles.

Proof: See Appendix E.

Corollary 11 shows that the number of iterations needed to reach convergence has an inverse quadratic relation with the

communication failure probability q. The larger the q, the greater number of iterations the D-AL may need to reach convergence. Note that Corollary 11 discusses the relations between the number of iterations and the disconnection probability q in an application scenario with a given number of participating vehicles m. If we are comparing the scenarios with different numbers of participating vehicles, we could easily adapt Corollary to conclude that the upper bound of the number of iterations has a quadratic relation with the number of participating vehicles m. Numerical experiments confirm our findings from Corollary 11. As will be shown in Sec 6, the convergence rate of the D-AL algorithm dramatically slows down as the disconnection probability q of individual vehicles increases.

5.2.3. Acceleration Scheme (aD-AL)

The above sub-sections show that though D-AL guarantees to converge under random communication failures, its convergence rate would decrease as the vehicle disconnection possibility increases. Then, we suspect that the D-LA won't satisfy the online routing application of the CeRM under high communication failure scenarios. For example, our experimental results show that the computation time under the vehicle disconnection probability of 0.2 is 2-3 times higher than under well-connected conditions, which takes more than a minute for scenarios with 1500 vehicles. To improve the solution algorithm's resilience in the computation performance under imperfect wireless communication scenarios, this sub-section proposes an acceleration scheme that could expedite the convergence rate by simply changing the number of tasks assigned to each individual vehicle. We refer to this variance as the accelerated distributed Augmented Lagrangian (aD-AL). We prove that the upper bound of the number of iterations needed to reach convergence would decrease under aD-AL compared with D-AL and discuss how this would affect the overall computation time.

Specifically, in aD-AL, every individual vehicle is assigned d computation tasks (we discuss the range of d in Remark 13) in consecutive order, i.e., vehicle v_i are assigned the following d computation tasks: ∇f_{v_i} , $\nabla f_{v_{i+1}}$, ..., $\nabla f_{v_{i+d-1}}$. The task assignment can be expressed as an $m \times m$ assignment matrix A, where the element $a_{i,j}$ (the element in the i'th row and j'th column) is 1 when the computation task ∇f_{v_i} is assigned to vehicle v_i and 0 otherwise. The column of A denoted as A_i represents the tasks sent to vehicle v_i , i.e.,

$$A_j = \left\{ \begin{array}{l} \left(0_{j-1}, 1_d, 0_{m-(j-1)-d}\right)^T, \ if \ m-(j-1) \geq d \\ \left(1_{d-(m-(j-1))}, 0_{m-d}, 1_{m-(j-1)}\right)^T, \ if \ m-(j-1) < d \end{array} \right.$$

Denote a $m \times (m-s)$ matrix W as the assignment matrix for well-connected vehicles, where s is the number of disconnected vehicles and the column W_i of W is taken from A when the corresponding vehicle is well connected. Then the approximated gradient under the acceleration scheme

$$G_a = \frac{m}{(m-s)d} \nabla \mathcal{F}^T \mathbf{W} \mathbf{1}_{m-s}, \tag{21}$$

where $\nabla \mathscr{F} = (\nabla f_{\nu_1}, ..., \nabla f_{\nu_m})^T$ is the column vector.

We next prove Lemma 12 to demonstrate that the variance of the gradient approximation error under aD-AL is bounded. This result will assist us to discuss the merit of aD-AL in Lemma 13.

Lemma 12. Variance of the gradient approximation error ϕ_{aD-AL} under the acceleration scheme measured by $E(\parallel G_a - \nabla \mathscr{L} \parallel^2)$ is bounded, i.e.,

$$\phi_{aD-AL} = E(\|\mathbf{G}_a - \nabla \mathcal{L}\|^2) \le \left(mq^m + \frac{2mq}{(1-q)d}\right) \|\nabla \mathcal{T}\|^2$$

Proof: See Appendix F.

Remark 13. For our application, the number of tasks assigned to each individual vehicle is at least 1, i.e., $d \ge 1$. Thus, Lemma 12 can be further developed and gets $\phi_{aD-AL} \le \left(mq^m + \frac{2mq}{(1-q)d}\right) \|\nabla \mathcal{F}\|^2 \le m\left(q^m + \frac{2q}{1-q}\right) \|\nabla \mathcal{F}\|^2$. Compared with Lemma 7 that proves $\phi_{D-AL} \le m\left(q^m + \frac{2q}{1-q}\right) \|\nabla \mathcal{F}\|^2$, we conclude that the approximation error in aD - AL has a smaller upper bound than that under D - AL. Then from Theorem 10, the number of iterations needed to reach certain solution accuracy under the aD-AL is likely to be smaller than that under the D-AL. However, this does not necessarily indicate that the aD-AL has a shorter overall computation time. While the convergence rate increases (the number of iterations to reach convergence decreases), the time for each iteration increases because each individual vehicle undertakes more tasks in the aD-AL than in the D-AL and needs more time to compute the assigned tasks in an iteration. In other words, there is a trade-off between the convergence rate and the time individual vehicles take to compute the assigned tasks. If the number of tasks assigned to each individual is $\frac{m}{m-s}$, where s is the number of disconnected vehicles, the CP can always receive full information of the gradient $\nabla \mathcal{L}$ for solving the MP - S (14) from connected vehicles by following our proposed task assignment plan defined by matrix A (under the assignment plan of matrix A, every task is assigned to d vehicles. So, if $d \ge \frac{m}{m-s}$, no task will be missing). Thus, in order to save computation time, the number of tasks d assigned to individual vehicles should be no larger than $\frac{m}{m-s}$. In the next section, we will show that by setting an appropriate number of tasks assigned to individual vehicles, the proposed aD-AL could expedite the overall computation time of the solution algorithm under high disconnection probabilities.

6. Numerical Experiment

This study conducts numerical experiments to demonstrate the efficiency of the D-AL and aD-AL algorithms and the efficacy of the

CeRM. Specifically, our experiments investigate three aspects: (1) the computation efficiency and convergence pattern of the D-AL algorithm; (2) the system cost reduction brought by the CeRM compared with benchmarks (IR, uoER, SOR) routing mechanisms; (3) how the CeRM affect the individual rationalities and the flow patterns in the network; (4) the robustness of the D-AL algorithm and the performance of the accelerated D-AL (aD-AL) under random communication failures. In addition, this section discusses how the CeRM can be applied to larger networks with a greater number of vehicles.

6.1. Experiment Settings

The experiments are conducted upon the topology of the Sioux Falls city network, which consists of 24 nodes and 76 links (Yang, 1999) and has been widely used as a testbed in the transportation field. The standard BPR function is adopted to capture link travel

time with the given flow, i.e., $c_l(f_l) = t_0^l \left(1 + 0.15 \left(\frac{f_l}{k_l}\right)^4\right)$, where t_0^l and k_l is the free-flow travel time and capacity of link l separately.

Vehicles represented by a three tuple (OD, α, β) are generated randomly with OD denoting the origin-destination pair and $\alpha, \beta \in [0, 1]$ being personal parameters used in the multinomial logit choice model as defined in (5). Each vehicle ν has two possible routes found by the k-shortest paths algorithm (Yen, 1971) under current (initial) traffic conditions. Detailed parameters used in the D-AL algorithm include: penalty updating parameter $\gamma_c = 10$; Constraint feasibility comparison parameter $\gamma_m = 0.7$; first order optimality tolerance $\varepsilon_m = 0.01$; feasibility tolerance $\varepsilon_c = 0.01$; Initial Lagrangian multiplier $\lambda_0 = 1$; Initial penalty $p_0 = 1$; initial step size $\bar{\alpha} = 1$; Armijo parameter $\omega = 0.5$, $\omega = 0.01$.

To measure the algorithm's efficiency, we implement the proposed D-AL algorithm in MATLAB R2020a and compare it with the SQP-based MATLAB solver since Sequential Quadratic Programming (SQP) is commonly used to solve nonconvex large-scale optimization problems. In addition, it has been used by recent works such as (Papadopoulos et al., 2021) to solve nonconvex problems in routing problems. To measure the routing mechanism's efficacy, we compare the system cost of the CeRM with that of (i) IR, by which each vehicle conducts one snapshot best response to real-time traffic information, (ii) uoER, by which the route choices of the vehicles are coordinated to a snapshot equilibrium resolution, and (iii) SOR, by which vehicles' route choices are systematically manipulated toward the minimum system cost. The experiments are conducted on the laptop with processor: Intel® Core™ i5-8300H CPU @ 2.30GHz.

6.2. Computation performance of D-AL

To demonstrate the proposed algorithm's computation performance, we run 14 traffic scenarios with the number of qualified participating vehicles increasing from 200 to 1500 by an increment of 100. Each scenario was run ten times and then we took the average performance to reduce contingency and randomness.

Fig. 2 displays the convergence pattern under the cases of 500, 1000, and 1500 vehicles. It indicates that the objective function drops quickly in the early period (when the penalty is small), fluctuates a little bit, then enters a flat district and stays stable (as penalty increases), which coincides with the typical convergence pattern of the Augmented Lagrangian algorithm.

Fig. 3 shows the average computation time for D-AL and SQP as the number of vehicles increases. It demonstrates that the SQP solver becomes computationally intractable (i.e., computation time is larger than 6000 seconds, which cannot adapt to online routing requirements) when the number of vehicles exceeds 800. The coefficient of variation for the computation time of the D-AL ranges between 0.19 to 0.43, with a maximum computation time of 28.7 sec happened in the scenario with 1500 vehicles. The D-AL dramatically outperforms SQP in all scenarios and we conclude that it could satisfy the fast computation need for an online navigation

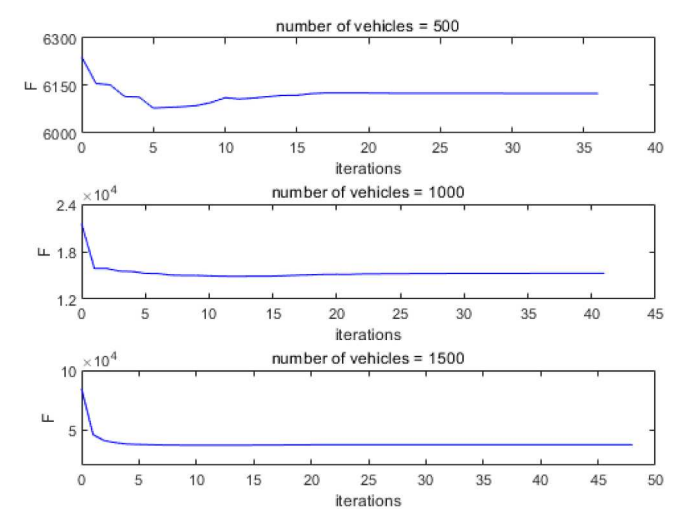


Fig. 2. Convergence pattern under different numbers of vehicles.

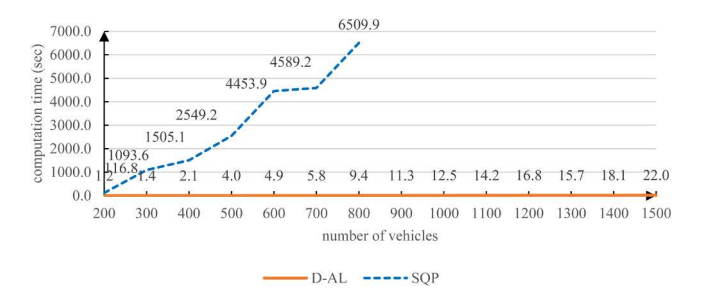


Fig. 3. Computation time under different numbers of vehicles.

service (i.e., handle a scenario with more than a thousand vehicles by an average leading time smaller than 22 seconds). It's worth noting that it is not proper to compare the computation time of the CeRM to that of the IR mechanism applications such as Google Map or Waze, since the formal one seeks to coordinate the routing decision of a group of vehicles, which is highly complicated and time-consuming, while the latter one only determines individual vehicles' route choices independently without coordination. To conclude, the D-AL algorithm shows stable convergence quality and is far more efficient than the traditional SQP algorithm regarding convergence speed. The computation performance of the D-AL can satisfy the need for a realistic online navigation service with a greater number of vehicles.

6.3. System Performance of the CeRM

This section further investigates the effectiveness of the CeRM in mitigating traffic congestion, while sustaining individual vehicles'' trip interest. The proposed D-AL is used to calculate the routing guidance under the CeRM. The system cost resulting from the collective route choices under the CeRM is compared with three benchmarks: IR. uoER, and SOR. The detailed formulations of these benchmarks are shown in Appendix D. Fourteen scenarios of experiments are conducted, in which the number of vehicles increased from 200 to 1500 with an increment of 100. Similar to the above, every scenario is run ten times to reduce the effect of randomness in the presented results. The coefficient of variation for different scenarios ranges between 0.018 to 0.027, which is very small and shows that the CeRM has stable system performance.

The experiment results are shown in Figs. 4 and 5. Fig. 4 shows the system cost comparison between IR and the CeRM, and Fig. 5

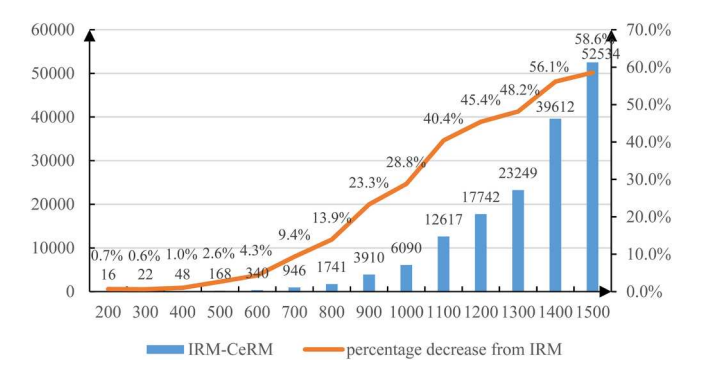


Fig. 4. System cost comparison between IR and CeRM.

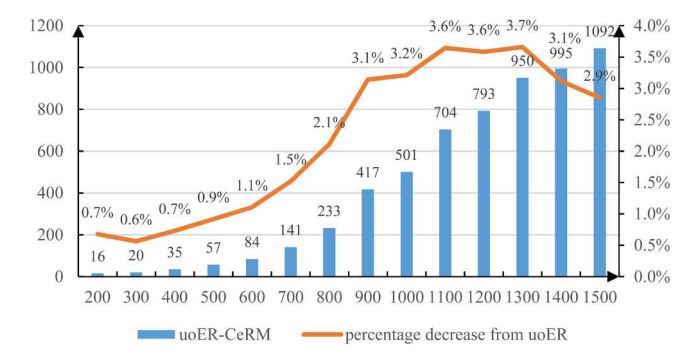


Fig. 5. System Cost comparison between uoER and CeRM.

 Table 4

 System performance under different numbers of vehicles.

Number of Vehicles	Δ_{CeRM}	$\Delta_{\mathbf{uoER}}$	$\Delta_{ ext{IR}}$	Number of Vehicles	Δ_{CeRM}	$\Delta_{\mathbf{uoER}}$	$\Delta_{ ext{IR}}$
200	72.74	88.40	88.41	900	589.15	1006.36	4498.82
300	110.34	130.51	132.34	1000	651.79	1152.41	6742.16
400	155.29	190.40	203.74	1100	663.79	1367.56	13280.52
500	242.11	299.35	410.44	1200	571.55	1364.15	18313.46
600	305.83	389.87	645.76	1300	575.57	1526.05	23824.54
700	441.50	582.75	1387.15	1400	440.08	1435.10	40052.14
800	526.70	759.24	2268.00	1500	443.80	1535.47	52978.12

shows the same comparison between the uoER and CeRM. Define Z_{CeRM} , Z_{IR} , Z_{UoER} , Z_{SOR} to be the system cost under the CeRM, IR, uoER, and SOR, respectively. The blue bars show the amount of the system cost reduction by the CeRM from the benchmark mechanisms, and the orange line shows the percentage of the system cost reduction as comparing the CeRM with IR or uoER, i.e., $\frac{Z_{IR}-Z_{CeRM}}{Z_{IR}}$ and $\frac{Z_{uoER}-Z_{CeRM}}{Z_{uoER}}$. It can be seen that the system cost of the CeRM is always lower than that under IR and uoER. As the number of vehicles increases, the system cost reduction by the CeRM increases. In congested scenarios, the system cost could be reduced by around 55% compared with IR and approximately 3.6% compared with uoER.

We also compare the system performance of the CeRM, IR, and uoER by measuring how much their induced system costs are higher than the System Optimum (SOR) cost, i.e., compare $\Delta_{CeRM} = Z_{CeRM} - Z_{SOR}$, $\Delta_{IR} = Z_{IR} - Z_{SOR}$ and $\Delta_{uoER} = Z_{uoER} - Z_{SOR}$. Given that SOR represents the best system performance, the smaller Δ is, the better the resulting system performance it represents. Table 4 clearly shows that the CeRM approaches the system optimum cost closely and it outperforms IR and uoER under all scenarios. To conclude, the CeRM pushes the snapshot traffic resulting from widely used IR to a more systematically efficient state. It proves to be efficient in reducing traffic congestion at a systematic level.

We further conduct a numerical experiment to demonstrate how would the levels of background traffic affect the performance of CeRM. Specifically, we test 10 scenarios each with a total of 1000 vehicles. The number of CeRM participating vehicles increases from 100 to 1000 with a step size of 100, which represents the penetration rate ranging from 10% - 100%. Each scenario is tested 10 times to reduce the effect of randomness. The experiment results in Fig. 6 show that as the penetration of the CeRM participating vehicles is small, the performance of the CeRM and IRM would be close. As the penetration rate increases, the effect of CeRM to reduce traffic congestion and system cost would become more obvious. The results also show that the system cost under the CeRM is always smaller than under the IRM, which validates the conclusion that the proposed CeRM outperforms the traditional IRM regarding system optimality.

6.4. Flow Patterns and Individual Rationality in the CeRM

This section first analyzes how the CeRM influences the traffic flow on the network. Figs. 7, 8 and 9 compares the heatmaps of the traffic flow on each link under routing mechanisms of IR, uoER, CeRM, and SOR in scenarios with 500, 1000, and 1500 vehicles. The darker the color, the more traffic there is on a link. We normalized the color (the volume of the flow) along each column to better compare the relative volume of the traffic flow on a link under different routing mechanisms. Figs. 7-9 show that both IR and SOR have quite **uneven** flow distributions on the network. Due to limited information provision, travelers in IR will pour into the seemingly smallest travel time routes based on given traffic information. While in SOR, drivers are assigned to routes that they are less likely to take in IR to minimize the system travel time, resulting in darker colors on links that are relatively less used in IR. On the contrary, the flows of uoER and CeRM are relatively evenly distributed on the network. By co-considering individual rationality and system performance, both uoER and CeRM can be seen as a trade-off between IR and SOR. While uoER directs some of the flow from the congested links in IR (links with darker colors) to other links to reduce congestion, CeRM goes one step further and pushes the traffic to be more systematically efficient. It can be seen in Figs. 7-9. that the flow distribution of CeRM is closer to SOR than uoER. The links that have darker colors in SOR are also darker in CeRM than in uoER, while the links that have lighter colors in SOR are also lighter in CeRM than in uoER.

Secondly, this section demonstrates travelers' rationality ratio under different routing mechanisms. It is measured by the ratio

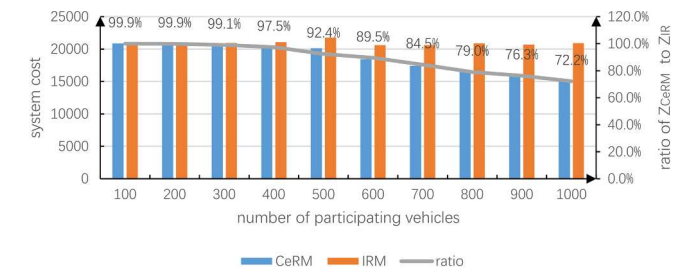


Fig. 6. System cost comparison of CeRM and IRM under different penetration rate.

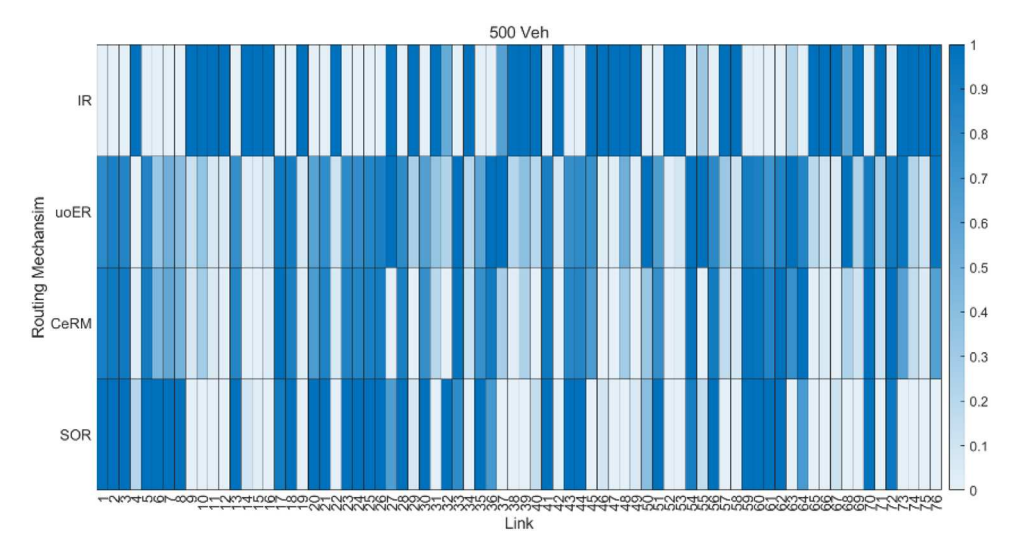


Fig. 7. Flow heatmap of 500 vehicles.

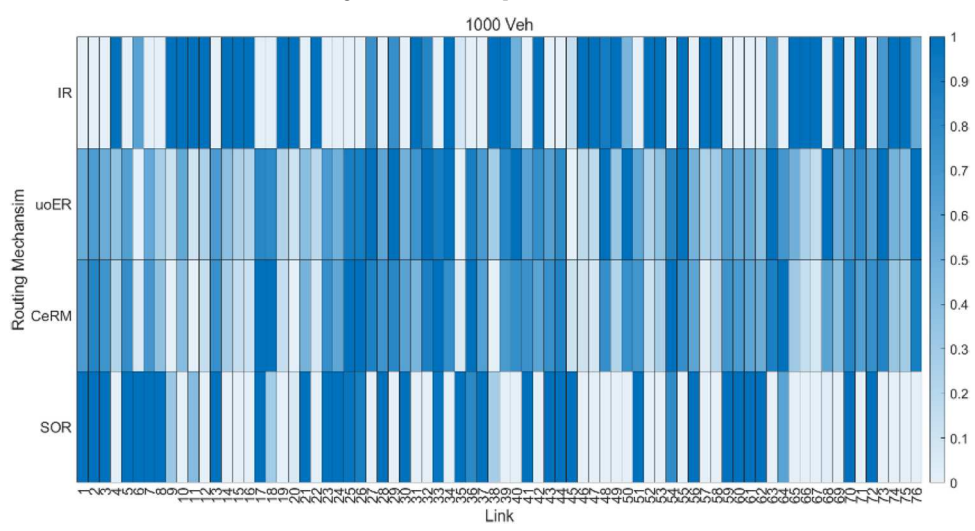


Fig. 8. Flow heatmap of 1000 vehicles.

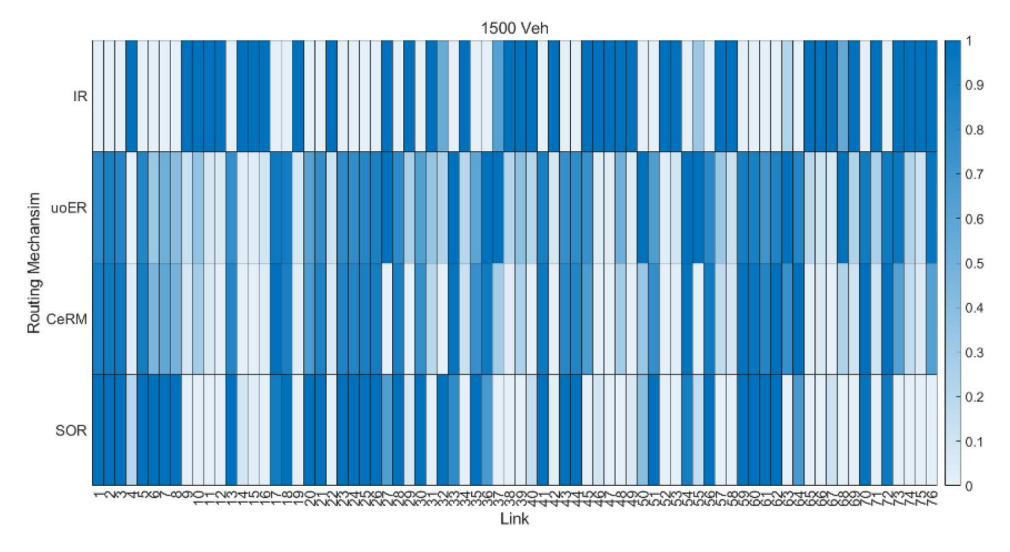


Fig. 9. Flow heatmap of 1500 vehicles.

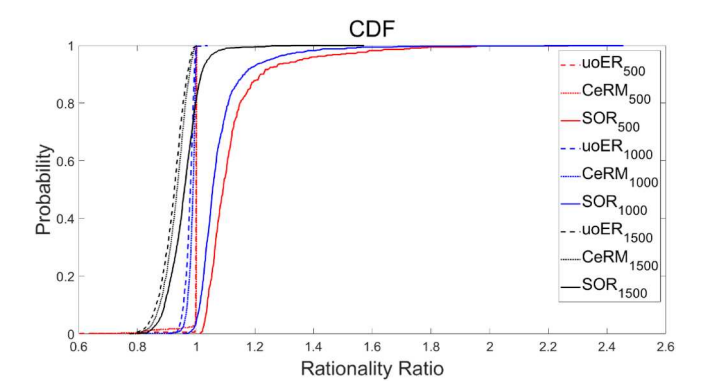


Fig. 10. CDF of Rationality ratio under different routing mechanisms.

between the expected disutility of following the routing mechanism and the expected disutility of unilaterally deviating and sticking to their initial routing preference by responding to given real-time traffic information. If the ratio is larger than 1, then following the recommended route preference violates the rationality of the traveler since he/she would be better off by deviating from the recommended routing preference. Fig. 10 presents the cumulative distribution of travelers' rationality ratio under uoER, CeRM, and SOR in scenarios with 500, 1000, and 1500 vehicles. We can see that SOR leads to more rationality violations than uoER and CeRM under all scenarios. For example, SOR leads almost all vehicles in the scenario of 500 vehicles and nearly 20% of vehicles in the scenario of 1500 vehicles to experience a rationality violation (rationality ratio larger than 1). While uoER and CeRM can successfully sustain users' rationality (rationality ratio smaller or equal to 1) under all three scenarios. In addition, it can be observed that the curve of uoER stays slightly on the left of the curve of the CeRM. It indicates that the average rationality ratio resulting from the uoER is smaller than that from CeRM. This is because uoER keeps selfish routing decisions without an explicit system performance objective, which is integrated into the CeRM through the correlated equilibrium. Therefore, CeRM leads to better system performance than uoER, while they preserve individuals' rationality (rationality ratio smaller or equal to 1).

6.5. Convergence Robustness of D-AL and Computation Resilience of aD-AL

This section demonstrates the convergence robustness of the D-AL against random communication failures and the effectiveness of the aD-AL in accelerating the computation performance (i.e., improving the resilience of the solution algorithm against communication failures). Figs. 11, 12 and 13 plot the computation time of the D-AL and aD-AL under the problem size equal to 500, 1000, and 1500 vehicles for the successful communication probabilities ranging from 0.8 to 1 with an increment of 0.02. According to the discussion in Remark 13, since it's likely that more than half of the vehicles are connected, the number of tasks assigned to each vehicle is set to be 2 in the adopted aD-AL, i.e., d=2. Every scenario is run ten times to reduce the effect of randomness. The result shows that the D-AL is robust to communication failures and could converge under different levels of communication probabilities. However, the computation time of the D-AL would increase violently as the communication probabilities decreases. On the contrary, the computation time of the aD-AL is relatively stable, which is much smaller than in the D-AL when the communication probabilities are small (i. e., the failure probability is large), while it is close to D-AL when communication probabilities are high. In addition, the "breaking point" (the red rectangular in the figure, which indicates the communication probability that the D-AL starts to perform equal to or slightly better than aD-AL) would become larger as the number of vehicles increases. This is because both D-AL and aD-AL has fast convergence rate when disconnection probabilities are small. In these circumstances, the time for calculating extra assigned tasks in aD-AL exceeds the time saved from having a faster convergence rate (as indicated in Remark 13), thus making aD-AL perform slightly worse than D-AL. The "breaking point" would become larger as the number of vehicles increases. This is because there will be more

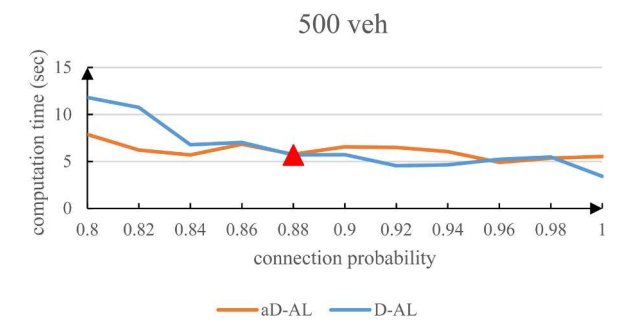


Fig. 11. Computation time under 500 vehicles.

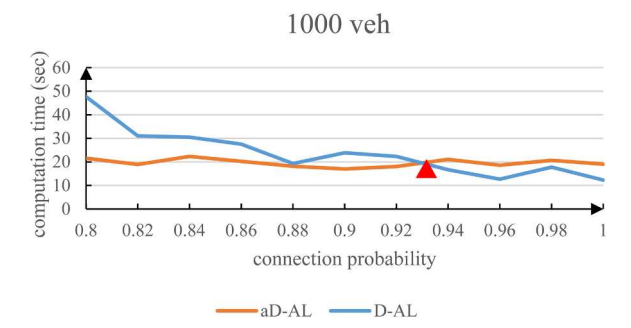


Fig. 12. Computation time under 1000 vehicles.

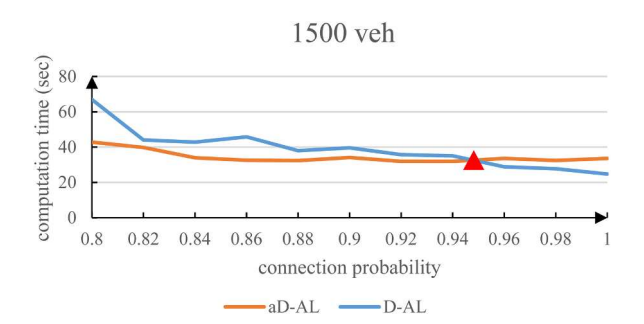


Fig. 13. Computation time under 1500 vehicles.

information loss in the scenario with more vehicles, even with the same level of connection probability. (As shown in Lemma 7, increasing the number of vehicles m will increase the approximation error ϕ_{D-AL}). Accordingly, the computation time saved from the accelerated convergence rate in aD-AL will be more remarkable. This observation gives favor to using aD-AL in navigation scenarios with a larger number of vehicles since its computation performance is more reliable under the high likelihood of communication failures.

6.6. Applicability to Larger Networks and More Vehicles

While the above numerical experiments are conducted on the Sioux Falls network with 200 - 1500 vehicles, CeRM can be easily applied to larger networks with more vehicles. This sub-section first analyzes the complexity of the CeRM model, demonstrate that network size is not the key factor to affect the computation performance, and then discusses how CeRM could be used in a bigger instance with more participating vehicles.

Firstly, it should be noted that the decision variables of the CeRM model in Eq. (8.1) – Eq. (8.5) are the routing probabilities $p_s^{v,i}$ for every vehicle v=1,...,m and the candidate path $i=1,...,k^v$. The number of decision variables is then $\sum_{v=1}^m k^v$. In addition, the number of complicated rationality constraints (Eq. (8.2)) relates to the number of vehicles (one for each vehicle). With that said, the complexity of the CeRM is mostly related to the number of participating vehicles and the number of candidate paths considered by each vehicle. The size of the network (number of links in the network) would not affect the complexity of our problem very much. To verify our complexity analysis, we conducted numerical experiments on the Eastern Massachusetts (EMA) network (74 nodes and 258 links) and the Winnipeg network (1057 nodes and 2535 links), which is much larger than the Sioux Falls network (24 nodes and 76 links). The number of vehicles ranges from 200 to 1500 and all other parameters are the same as in the numerical experiments conducted on the Sioux Falls network. The results in Fig. 14 show that the computation time to solve our CeRM problem does not increase much as the network size increases.

Secondly, the CeRM can be easily applied to scenarios with a larger number of vehicles by combining clustering techniques. It's worth noting that if travelers are completely non-overlap (routes in their candidate route sets do not overlap spatially and temporally), they will have no potential to coordinate and improve traffic efficiency. For example, such non-overlap can be found when drivers are traveling in different districts of a city, drivers are traveling in different time periods during the day, etc. In fact, though the annual average daily traffic volume on each road segment in the Orlando area (Orange County, FL) can reach 77000, the peak hourly volume only ranges from several dozen to no more than 3300 in each road segment in one direction (Orange County Traffic Counts). The number of vehicles that have strong potential to coordinate would be even less. Such spatially and temporally different distribution of travelers makes it unnecessary to conduct CeRM on all travelers in one shot. With this logic, there's another line of research (Peng and Du, 2021; Peng and Du, 2022) that proposed to separate the travelers into multiple sub-groups and implement routing coordination mechanisms separately in each sub-group. Specifically, (Peng and Du, 2021) studied how to quantify the routing coordination

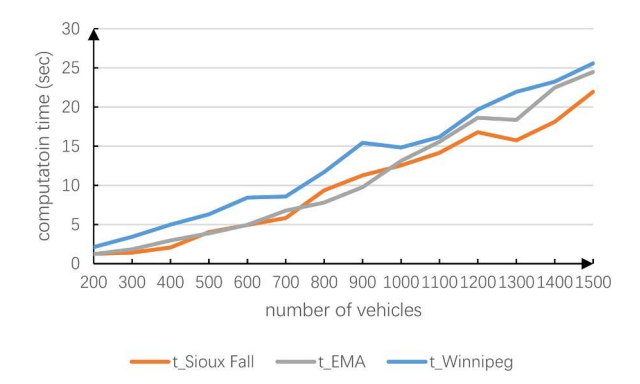


Fig. 14. Computation time in Sioux Falls and EMA.

potential between travelers, which measures the potential opportunity that they will use the same road links in the same future time interval. Efficient clustering algorithms (Peng and Du, 2021; Peng and Du, 2022) are then developed to partition travelers into sub-groups according to their coordination potential, so that the coordination potential is large within the sub-group and small between different sub-groups. The experimental results showed that such an approach reduces computation load significantly while incurring only minor sacrifice in the system performance as compared to conducting routing mechanisms for all travelers in one shot. Take the Orlando area as an example, after forming sub-groups, the number of travelers within each sub-group would lie between the number of vehicles tested in our experiments, which justifies the use case we adopted. Since this research has already been validated and published, this study won't repeat the experiments here.

7. Conclusion

This study designs a correlated routing mechanism that calculates and provides online routing guidance for vehicles with onboard computing and communication devices. By exploiting information discrepancies between individual vehicles and the CP, the proposed mechanism drives the snapshot equilibrium route choice of a group of vehicles toward a more systematic optimal condition while still preserving the individual's selfish nature. By following the routing guidance offered by the CP, every driver would get better off (at least not worse off) compared to their initial preference based on current traffic information. Furthermore, this study proposes the D-AL, an effective distributed algorithm to quickly solve the routing problem for an online real-time navigation service. The convergence properties and robustness of the D-AL are proved theoretically. By noticing the convergence rate of the D-AL degrades dramatically as the disconnection probability increases, this study also proposed an acceleration scheme that could expedite the computation speed and thus improve the resilience of the solution algorithm in the computation performance degradation under high disconnection probabilities. The conducted numerical experiments demonstrate the merits of the D-AL and aD-AL in both the convergence speed and robustness against random communication failures. The experimental results also indicate that the CeRM drives the traffic equilibrium to a state better than that under IR and uoER regarding the objective of the system cost. To the best of our knowledge, this is one of the first studies to design an online routing mechanism based on correlated equilibrium and distributed optimization to mitigate network traffic congestion. We are also among the pioneering studies to investigate the robust and resilient routing mechanism against communication failures. The methodology and findings of this study will significantly contribute to traffic congestion mitigation areas in both literature and practice.

There are several possible extensions stemming from this work. For example, the convergence speed of the D-AL now heavily depends on the computation load of searching the step size. The future study can explore the distributed step size calculation scheme to improve the convergence efficiency dramatically. In addition, like most existing transportation studies adopting mixed strategy games (Wu, Yin, and Lawphongpanich, 2011; Zhang et al., 2014; Du, Han, and Li, 2014), this study assumes travelers' route choice behavior can be modeled by logit choice models. However, in reality, travelers' behavior choice uncertainties may not be completely captured by discrete choice models, which would bring in errors in estimating their expected utility and result in compliance issues. Therefore, a possible future work is to incorporate approaches from behavioral and experimental games to develop reliable implementation schemes for the mixed strategy routing mechanism to ensure traveler's compliance with the suggested route. We will investigate these new challenges in our future studies.

Author Statements

The authors confirm contributions to the paper as follows: Lili Du (LD) initiated the research idea and led the main methodologies development. Yuqiang Ning (YN) contributes to the development of the technical details in mathematical development, analysis, and experiments under the supervision of LD. Both authors reviewed the results and approved the final version of the manuscript.

Declaration of Competing Interest

The authors declare that they have no known competing financial interests or personal relationships that could have appeared to influence the work reported in this paper.

Acknowledgement

This research is partially supported by National Science Foundation, award CMMI 1818526 (Previous: 1554559) and UTC STRIDE center H3 project.

Appendix

Appendix A

Lemma 13. The optimization problem has a convex objective function and a nonconvex feasible region.

Proof: To check the convexity of the objective function, we exam its Hessian and noticed the Hessian of Z is positive definite.

$$H(Z) = \begin{bmatrix} \frac{\partial^2 Z}{\partial p_s^{v_1,i_1} \partial p_s^{v_1,i_1}} & \frac{\partial^2 Z}{\partial p_s^{v_1,i_1} \partial p_s^{v_1,i_2}} & \cdots & \frac{\partial^2 Z}{\partial p_s^{v_1,i_1} \partial p_s^{v_m,i_{k^m}}} \\ \frac{\partial^2 Z}{\partial p_s^{v_1,i_2} \partial p_s^{v_1,i_1}} & \frac{\partial^2 Z}{\partial p_s^{v_1,i_2} \partial p_s^{v_1,i_2}} & \cdots & \cdots \\ \cdots & \cdots & \cdots & \cdots \\ \frac{\partial^2 Z}{\partial p_s^{v_m,i_{k^m}} \partial p_s^{v_1,i_1}} & \frac{\partial^2 Z}{\partial p_s^{v_m,i_{k^m}} \partial p_s^{v_1,i_2}} & \cdots & \frac{\partial^2 Z}{\partial p_s^{v_m,i_{k^m}} \partial p_s^{v_m,i_{k^m}}} \end{bmatrix}$$

$$= \Omega \begin{bmatrix} 2c_{1}^{'}(f_{s}^{L}) + f_{s}^{L}c_{1}''(f_{s}^{L}) & & & \\ & 2c_{2}^{'}(f_{s}^{L}) + f_{s}^{L}c_{2}''(f_{s}^{L}) & & \\ & & & & \\ & & & & \\ & & & & \\ & & & & \\ & & & & \\ & & & & \\ & & & & \\ & & & & \\ & & & & \\ & & \\ & & & \\$$

where Ω is the link-path relation matrix, i.e., $\Omega = \left(\begin{array}{cccc} \delta^1_{\nu_1,i_1} & \delta^2_{\nu_1,i_1} & \dots & \delta^n_{\nu_1,i_1} \\ \delta^1_{\nu_1,i_2} & \delta^2_{\nu_1,i_2} & \dots & \delta^n_{\nu_1,i_2} \\ \dots & \dots & \dots & \dots \\ \delta^1_{-} & \delta^2_{-} & \dots & \delta^n_{-} & \dots & \delta^n_{-} \end{array} \right).$

Since the link cost function is strictly increasing and convex according to assumption 6, c/ and c/' would be positive. Thus, every element in matrix Λ is positive. Given any diagonal matrix Λ with positive elements, for any vector x and matrix M, $x^TM\Lambda M^Tx =$ $(M^Tx)^T\Lambda(M^Tx) > 0$ must hold. Hence, the hessian matrix H(Z) is positive definite.

Next, we check the rationality constraint's convexity and notice that the Hessian of rationality constraints is indefinite. More exactly, we first calculate the elements in the Hessian and then prove it is neither positive (semi) definite nor negative definite.

The first derivatives of the rationality constraint of vehicle v^* are:

$$\begin{split} \frac{\partial r_{v^*}}{\partial p_s^{v^*,i^*}} &= \sum_{L \in r^{v^*,i^*}} c_L (f_s^L) + \frac{1}{\beta_{v^*}} \left(1 + \ln(p_s^{v^*,i^*})\right) + \sum_{i=1}^{k_{v^*}} p_s^{v^*,i} \sum_{L \in r^{v^*,i}} c_L' (f_s^L) \delta_{v^*,i^*}^L, \ i^* = 1, ..., k^{v^*} \\ \frac{\partial r_{v^*}}{\partial p_s^{v^*,i}} &= \sum_{i=1}^{k_v^*} p_s^{v^*,i} \sum_{L \in r^{v^*,i}} c_L' (f_s^L) \delta_{v^*,i^*}^L - \sum_{i=1}^{k_v^*} p_s^{v^*,i} \sum_{L \in r^{v^*,i}} c_L' (f_s^L) \delta_{v^*,i^*}^L, \ i^* = 1, ..., k^{v^*} \end{split}$$

$$\frac{\partial r_{v^*}}{\partial p_{s}^{v',i}} = \sum_{i=1}^{k_{v^*}} p_{s}^{v^*,i} \sum_{L \in r^{v',i}} c_L'(f_s^L) \delta_{v',i'}^L - \sum_{i=1}^{k_{v^*}} p_o^{v^*,i} \sum_{L \in r^{v',i}} c_L'(f_o^L) \delta_{v',i'}^L, v' \neq v^*, \quad i' = 1, ..., k^{v'}$$

the elements in the Hessian matrix of the rationality constraint of vehicle v^* are:

$$\begin{split} &\frac{\partial r_{v^*}}{\partial p_{s}^{v^*,i^*}\partial p_{s}^{v^*,i^*}} = 2\sum_{L \in r^{v^*,i^*}} c_L'(f_s^L) \delta_{v^*,i^*}^L + \sum_{i=1}^{k_v^*} p_{s}^{v^*,i} \sum_{L \in r^{v^*,i}} c_L''(f_s^L) \delta_{v^*,i^*}^L + \frac{1}{\beta_{v^*} p_{s}^{v^*,i^*}}, \ i^* = 1, \dots, k^{v^*} \\ &\frac{\partial r_{v^*}}{\partial p_{s}^{v^*,i^*}\partial p_{s}^{v^*,i}} = 2\sum_{L \in r^{v^*,i^*}} c_L''(f_s^L) \delta_{v^*,j}^L + \sum_{i=1}^{k_v^*} p_{s}^{v^*,i} \sum_{L \in r^{v^*,i}} c_L''(f_s^L) \delta_{v^*,i^*}^L \delta_{v^*,j}^L, \quad j \neq i^* \\ &\frac{\partial r_{v^*}}{\partial p_{s}^{v^*,i^*}\partial p_{s}^{v^*,i}} = 2\sum_{L \in r^{v^*,i^*}} c_L''(f_s^L) \delta_{v^*,j}^L + \sum_{i=1}^{k_v^*} p_{s}^{v^*,i} \sum_{L \in r^{v^*,i}} c_L''(f_s^L) \delta_{v^*,i^*}^L \delta_{v^*,j}^L, \quad j \neq i^* \\ &\frac{\partial r_{v^*}}{\partial p_{s}^{v^*,i^*}\partial p_{s}^{v^*,i}} = \sum_{L \in r^{v^*,i^*}} c_L''(f_s^L) \delta_{v',i^*}^L + \sum_{i=1}^{k_v^*} p_{s}^{v^*,i} \sum_{L \in r^{v^*,i}} c_L''(f_s^L) \delta_{v^*,i^*}^L \delta_{v^*,i}^L, \quad v' \neq v^*, \quad i' = 1, \dots, k^{v'} \\ &\frac{\partial r_{v^*}}{\partial p_{s}^{v',i^*}\partial p_{s}^{v^*,i}} = \sum_{L \in r^{v^*,i}} c_L''(f_s^L) \delta_{v',i^*}^L + \sum_{i=1}^{k_v^*} p_{s}^{v^*,i} \sum_{L \in r^{v^*,i}} c_L''(f_s^L) \delta_{v^*,i^*}^L \delta_{v',i^*}^L, \quad v' \neq v^*, \quad i' = 1, \dots, k^{v'} \\ &\frac{\partial r_{v^*}}{\partial p_{s}^{v',i}\partial p_{s}^{v^*,i}} = \sum_{i=1}^{k_v^*} p_{s}^{v^*,i} \sum_{L \in r^*,i} c_L''(f_s^L) \delta_{v',i^*}^L \delta_{v',i^*}^L, \quad v' \neq v^*, \quad i' = 1, \dots, k^{v'} \\ &\frac{\partial r_{v^*}}{\partial p_{s}^{v',i}\partial p_{s}^{v^*,i}} = \sum_{i=1}^{k_v^*} p_{s}^{v^*,i} \sum_{L \in r^*,i} c_L''(f_s^L) \delta_{v',i^*}^L \delta_{v',i^*}^L, \quad v' \neq v^*, \quad i' = 1, \dots, k^{v'} \\ &\frac{\partial r_{v^*}}{\partial p_{s}^{v',i}\partial p_{s}^{v',i}} = \sum_{i=1}^{k_v^*} p_{s}^{v^*,i} \sum_{L \in r^*,i} c_L''(f_s^L) \delta_{v',i^*}^L \delta_{v',i^*}^L, \quad v' \neq v^*, \quad i' = 1, \dots, k^{v'} \\ &\frac{\partial r_{v^*}}{\partial p_{s}^{v',i}\partial p_{s}^{v',i}} = \sum_{i=1}^{k_v^*} p_{s}^{v^*,i} \sum_{L \in r^*,i} c_L''(f_s^L) \delta_{v',i^*}^L \delta_{v',i^*}^L, \quad v' \neq v^*, \quad i' = 1, \dots, k^{v'} \end{cases}$$

Take a simplified scenario for the demonstration. Assume there are three simple routes (routes that contain only one link) 1, 2 and 3 connecting O and D, and there are only two vehicles a, b traveling in between. Vehicle a has three possible routes 1, 2 and 3, while vehicle b has only two possible routes 1 and 2. Denote the Hessian matrix as Φ , then for any vector x:

$$x\Phi x^{T} = x_{1}^{2} \left(\underbrace{2c_{1}^{'}(f_{s}^{1}) + p_{s}^{v_{a},i_{1}}c_{1}^{"}(f_{s}^{1}) + \frac{1}{\beta_{v_{1}}p_{s}^{v_{1},i_{1}}}}_{A} \right) + 2x_{1}x_{4} \left(\underbrace{c_{1}^{'}(f_{s}^{1}) + p_{s}^{v_{a},i_{1}}c_{1}^{"}(f_{s}^{1})}_{B} \right)$$

$$+ x_{2}^{2} \left(\underbrace{2c_{2}^{'}(f_{s}^{2}) + p_{s}^{v_{a},i_{2}}c_{2}^{"}(f_{s}^{2}) + \frac{1}{\beta_{v_{1}}p_{s}^{v_{1},i_{2}}}}_{C} \right)$$

$$+ 2x_{2}x_{5} \left(\underbrace{c_{2}^{'}(f_{s}^{2}) + p_{s}^{v_{a},i_{2}}c_{2}^{"}(f_{s}^{2})}_{D} \right)$$

$$+ x_{3}^{2} \left(\underbrace{2c_{3}^{'}(f_{s}^{3}) + p_{s}^{v_{a},i_{3}}c_{3}^{"}(f_{s}^{3}) + \frac{1}{\beta_{v_{1}}p_{s}^{v_{1},i_{3}}}}_{E} \right)$$

$$+ x_{4}^{2} \left(\underbrace{p_{s}^{v_{a},i_{1}}c_{1}^{"}(f_{s}^{1}) - p_{o}^{v_{a},i_{1}}c_{1}^{"}(f_{o}^{1})}_{F} \right)$$

$$+ x_{5}^{2} \left(\underbrace{p_{s}^{v_{a},i_{2}}c_{2}^{"}(f_{s}^{2}) - p_{o}^{v_{a},i_{2}}c_{1}^{"}(f_{o}^{2})}_{G} \right)$$

Take c_l to be the BPR function where $c_l = t_0^l \left(1 + 0.15 \left(\frac{f_l}{k_l}\right)^4\right)$. Then since f_l is strictly positive, c_l' and c_l'' will also be positive. And thus A, B, C, D, E > 0.

Thus, we have
$$x\Phi x^T\{$$
 ≥ 0 , $if \ x_3^2 < \frac{x_1^2A + 2x_1x_4B + 2x_2x_5D + x_2^2C + x_4^2F + x_5^2G}{E}$. So, the hessian matrix Φ is indefinite, and the ≥ 0 , $if \ x_4 \geq \frac{x_1^2A + 2x_1x_4B + 2x_2x_5D + x_2^2C + x_4^2F + x_5^2G}{E}$.

feasible region defined by the constraint is nonconvex. Q.E.D

Appendix B

Proof of Theorem 1:

We denote a solution point $P_s = \{p_s^{v,i}\} = X = (x_1, ..., x_{km})$ and $X^i = (x_1, ..., x_i + dx_i, ..., x_{km})$, then the numerical calculation of a single partial derivative for a vehicle in n-DS takes the form:

$$\frac{\partial \mathcal{L}}{\partial x_i} = \frac{\mathcal{L}(\mathbf{X}^i) - \mathcal{L}(\mathbf{X})}{dx_i} = \frac{\sum_{v=1}^m \nabla f_v(\mathbf{X}^i) - \sum_{v=1}^m \nabla f_v(\mathbf{X})}{dx_i}, i = k(v-1) + 1, \dots, kv.$$

In the contrast, the numerical calculation of a single partial derivative for a vehicle in c-DS takes the form:

$$\frac{\partial f_{v}}{\partial x_{i}} = \frac{f_{v}(\mathbf{X}^{i}) - f_{v}(\mathbf{X})}{dx_{i}}, i = 1, ..., km$$

An individual vehicle under c-DS has to compute km partial derivatives, while under n-DS has to compute k partial derivatives. Consider the time complexity it takes to numerically calculate $f_v(\mathbf{X})$ as l. Then the computation costs measured by the time complexity of vehicle j under c-DS and n-DS are given below:

c-DS time complexity: (km + 1)l

• the vehicle needs to calculate km different $\frac{\partial f_v}{\partial x_i}$, and thus needs to calculate $\underbrace{f_{v_j}(X^1), \dots, f_{v_j}(X^{km})}_{km}, \underbrace{f_{v_j}(X)}_{1}$

n-DS time complexity: (k + 1)ml

• the vehicle needs to calculate k different $\frac{\partial \mathcal{L}}{\partial x_i}$, and thus needs to calculate $\underbrace{\sum_{\nu=1}^m f_{\nu}(X^{k(j-1)+1})}_{k}, \dots, \underbrace{\sum_{\nu=1}^m f_{\nu}(X^{kj})}_{m}, \underbrace{\sum_{\nu=1}^m f_{\nu}(X)}_{m}$

Then, we claim a vehicle in *c*-DS undertakes $\frac{(k+1)ml-(km+1)l}{(k+1)ml} = \frac{1-\frac{1}{m}}{k+1}$ less workload than in *n*-DS. Q.E.D

Appendix C

Proof of Theorem 2:

Projecting a vector $Y = (y_1, ..., y_n)$ into the ε -probability simplex space equals to solving the optimization problem of:

$$\min_{X} \frac{1}{2} || X - Y ||^2$$

$$s.t. \quad X^T 1 = 1$$

$$\epsilon \le x_1, \dots, x_n$$
(22)

KKT conditions of the problem are:

$$\nabla_{x_i} \mathcal{L}(X^*, \lambda^*, \mu^*) = x_i - y_i + \lambda - \mu_i = 0, \quad i = 1, ..., n$$
 (19.1)

$$\nabla_{\lambda} \mathcal{L}(X^*, \lambda^*, \mu^*) = \sum_{i=1}^{n} x_i - 1 = 0$$
 (19.2)

$$\mu_i(\epsilon - x_i) = 0, \quad i = 1, ..., n$$
 (19.3)

$$\epsilon < x_i, \quad i = 1, ..., n$$
 (19.4)

$$\mu_i \ge 0, \quad i = 1, ..., n$$
 (19.5)

From above, we know that

$$\begin{cases} if \ x_i > \epsilon, \ then \ \mu_i = 0 \ and \ y_i - \lambda = x_i > \epsilon \\ if \ x_i = \epsilon, \ then \ \mu_i \ge 0 \ and \ y_i - \lambda = x_i - \mu_i = \epsilon - \mu_i \le \epsilon \end{cases}$$
(23)

(23) indicates that if $y_i \ge y_j$, then $x_i \ge x_j$. Without loss of generality, assume that Y has been sorted in descending order, and X is arranged using the same index, i.e.,

$$y_1 \ge y_2 \ge \dots \ge y_n$$

 $x_1 \ge x_2 \ge \dots \ge x_k > x_{k+1} = \dots = x_n = \epsilon$ (24)

Replacing (23) and (24) to (19.2), we have:

$$\sum_{i=1}^{n} x_i = \sum_{i=1}^{k} x_i + (n-k)\varepsilon = \sum_{i=1}^{k} (y_i - \lambda) + (n-k)\varepsilon = 1$$
 (25)

Then.

$$\lambda = \frac{\sum_{i=1}^{k} y_i + (n-k)\epsilon - 1}{k} \tag{26}$$

To this end, if we find the boundary index k, we could determine the value of λ and calculate the projected vector by:

$$x_i = \max\{y_i - \lambda, \epsilon\} \tag{27}$$

By substituting (27) to (19.1) – (19.5), It's easy to find that it would satisfy all the KKT conditions and would thus be the optimal solution to the problem (22).

Next, we show that step 3 of Algorithm 1 will successfully find the boundary index k, i.e., if k is the index found in step 3 of Al-

$$\text{gorithm 1, then } \begin{cases} y_j - \frac{\sum_{i=1}^{j} y_i + (n-j)\epsilon - 1}{j} > \epsilon, \ \forall j \leq k \\ y_j - \frac{\sum_{i=1}^{j} y_i + (n-j)\epsilon - 1}{j} \leq \epsilon, \ \forall j > k \end{cases}$$

Suppose that now we have found the largest index k, such that $y_k - \frac{\sum_{i=1}^k y_i + (n-k)\epsilon - 1}{k} > \epsilon$. Let $\lambda = \frac{\sum_{i=1}^k y_i + (n-k)\epsilon - 1}{k}$. Then,

1) for index $j \leq k$,

$$y_{j} - \frac{\sum_{i=1}^{j} y_{i} + (n-j)\epsilon - 1}{j} = \frac{jy_{j} - \sum_{i=1}^{j} y_{i} - (n-j)\epsilon + 1}{j} = \frac{jy_{j} + \sum_{i=j+1}^{k} y_{i} - \sum_{i=1}^{k} y_{i} - (n-j)\epsilon + 1}{j}$$
(28)

From (25), we have

$$\sum_{i=1}^{k} y_i = 1 + k\lambda - (n-k)\epsilon \tag{29}$$

Insert (29) into (28), we have

$$y_{j} - \frac{\sum_{i=1}^{j} y_{i} + (n-j)\epsilon - 1}{j} = \frac{jy_{j} + \sum_{i=j+1}^{k} y_{i} - k\lambda + (j-k)\epsilon}{j} = \frac{j(y_{j} - \lambda) + \sum_{i=j+1}^{k} (y_{i} - \lambda) + (j-k)\epsilon}{j} > \frac{j\epsilon + (k-j)\epsilon + (j-k)\epsilon}{j} = \epsilon$$

$$(30)$$

Note that the inequality in (30) results from that y is sorted in descending order, thus for $i \le k$, $y_i - \lambda \ge y_k - \lambda > \varepsilon$.

1) for index j > k, incorporate (29), we have

$$y_{j} - \frac{\sum_{i=1}^{j} y_{i} + (n-j)\epsilon - 1}{j} = \frac{jy_{j} - \sum_{i=1}^{k} y_{i} - \sum_{i=k+1}^{j} y_{i} - (n-j)\epsilon + 1}{j} = \frac{jy_{j} - \sum_{i=k+1}^{j} y_{i} - k\lambda + (j-k)\epsilon}{j}$$

$$= \frac{k(y_{j} - \lambda) + \sum_{i=k+1}^{j} (y_{j} - y_{i}) + (j-k)\epsilon}{j} \le \frac{k\epsilon + (j-k)\epsilon}{j} = \epsilon$$
(31)

Note that the inequality in (31) results from that y is sorted in descending order, thus for j > k, $y_j - \lambda \le \varepsilon$ and for i < j, $y_j - y_i \le 0$. Combining (30) and (31), we conclude that if we find the largest index k such that $y_k - \frac{\sum_{j=1}^k y_j + (n-k)\varepsilon - 1}{k} > \varepsilon$, then for index j < k, $y_j - \frac{\sum_{j=1}^l y_j + (n-j)\varepsilon - 1}{j} > \varepsilon$, for index j > k, $y_j - \frac{\sum_{j=1}^l y_j + (n-j)\varepsilon - 1}{j} \le \varepsilon$, and thus k would be the boundary index we need. Q.E.D

Appendix D

Proof of Lemma 5: The expectation of G can be expressed as

$$E(\mathbf{G}) = E\left(\frac{m}{m-s}\nabla \mathcal{F}^T \mathbf{B}\right) = \nabla \mathcal{F}^T E\left(\frac{m}{m-s}\mathbf{B}\right),\tag{32}$$

where s is the number of disconnected vehicles, $s = m - \sum_{i=1}^{m} b_i$ and $b_i = 1$ with probability 1 - q. When s = m (every vehicle is

disconnected), the CP cannot receive no gradient information from individual vehicles. Accordingly, the D-AL will skip this update by setting $\frac{m}{m-s}B = 0_m$. Then, $E(\frac{m}{m-s}B)$ could be derived as follows

$$E\left(\frac{m}{m-s}\boldsymbol{B}\right) = 0_m + E_{s < m} \begin{pmatrix} m \\ \frac{b_1}{b_2} \\ \vdots \\ b_m \end{pmatrix},\tag{33}$$

where

$$E_{s < m}\left(\frac{m}{m-s}b_i\right) = \sum_{s=0}^{m-1} \frac{m}{m-s} p(s|b_i=1)p(b_i=1) = \sum_{s=0}^{m-1} \frac{m}{m-s} \left(C_{m-1}^{m-s-1}q^s(1-q)^{m-s-1}\right)(1-q) = \sum_{s=0}^{m-1} \frac{m}{m-s} C_{m-1}^{m-s-1}q^s(1-q)^{m-s}$$

$$(34)$$

Where, $C_m^n = \frac{m!}{(m-n)!n!}$ is the combination formula. Thus, combining (33) and (34), we have

$$E\left(\frac{m}{m-s}\boldsymbol{B}\right) = 0_{m} + \sum_{s=0}^{m-1} \frac{m}{m-s} C_{m-1}^{m-s-1} q^{s} (1-q)^{m-s} 1_{m} = \sum_{s=0}^{m-1} C_{m}^{m-s} q^{s} (1-q)^{m-s} 1_{m} = \left(\sum_{s=0}^{m} C_{m}^{m-s} q^{s} (1-q)^{m-s} - C_{m}^{0} q^{m} (1-q)^{0}\right) 1_{m}$$

$$= (1-q^{m}) 1_{m}$$
(35)

Incorporate (35) into (32), we could then derive the expectation of G as follows

$$E(\mathbf{G}) = \nabla \mathcal{F}^T E\left(\frac{m}{m-s}\mathbf{B}\right) = \nabla \mathcal{F}^T (1-q^m) \mathbf{1}_m = (1-q^m) \sum_{i=1}^m \nabla f_{v_i} = (1-q^m) \nabla \mathcal{L} = \sigma \nabla \mathcal{L}$$
(36)

Clearly, $\sigma = 1 - q^m$ is a positive constant very close to 1, when m is large, and q is small. As stated in Remark 4, by simply multiplying the step size α_k with a constant scalar $\frac{1}{\sigma}$, the expectation of G can be seen as an unbiased estimator of $\nabla \mathcal{L}$, i.e., $E(G) = \nabla \mathcal{L}$. Q.E.D

Proof of Lemma 6: To conduct this proof, we first note that the norm of a $n \times n$ matrix is bounded if all entries in the matrix are bounded:

$$||A|| = \max_{x \neq 0} \frac{||Ax|||}{||x||} \le \max_{x \neq 0} \frac{\sqrt{n} ||Ax||_{\infty}}{||x||} \le \max_{x \neq 0} \frac{\sqrt{n} ||Ax||_{\infty}}{||x||_{\infty}} = \sqrt{n} ||A||_{\infty} = \sqrt{n} \max_{i} \sum_{i} |a_{ij}|$$

$$(37)$$

Then, recall from (10) that

$$\mathcal{L}(\boldsymbol{X}, \boldsymbol{\lambda}_{\boldsymbol{K}}, c_{\boldsymbol{K}}) = \underbrace{\sum_{L=1}^{n} f_{s}^{L} c_{L}(f_{s}^{L})}_{} + \frac{1}{2c_{K}} \sum_{v=1}^{m} (\max^{2} \{0, \lambda_{K}^{v} + c_{K} r_{v}(\boldsymbol{X})\} - \lambda^{v2}),$$

we can derive the entries in $\nabla \mathscr{L}$ as follows.

$$\left| \frac{\partial \mathscr{L}}{\partial p_{s}^{v^{*},i}} \right| \leq \sum_{l} \left| c_{l} (f_{s}^{L}) \left| \delta_{v^{*},i}^{L} + \sum_{\nu=1}^{m} \sum_{l} p_{s}^{\nu,i} \left| c_{l}^{'} (f_{s}^{l}) \left| \delta_{v^{*},i}^{l} \delta_{\nu,i}^{l} + \sum_{\nu=1}^{m} (c|r_{\nu}| + \lambda^{\nu}) \left| \frac{\partial r_{\nu}}{\partial p_{s}^{v^{*},i}} \right| \right|$$
(38)

Since $f_s^l = \sum_{\nu=1}^m \sum_{i=1}^{k^{\nu}} p_s^{\nu,i} \delta_{\nu,i}^l \in [0,m]$ and by Assumption 4, $c_l(f_s^l)$ and $c_l'(f_s^l)$ and $c_l'(f_s^l)$ are bounded. Since $\ln(p_s^{\nu,i})$ and $\frac{1}{p_s^{\nu,i}}$ is bounded when $p_s^{\nu,i} \ge \epsilon$ (see constraints (8.4)), r_{ν} and $\frac{\partial r_{\nu}}{\partial p_s^{\nu,i}}$ is bounded (see the equation of r_{ν} and $\frac{\partial r_{\nu}}{\partial p_s^{\nu,i}}$ in Appendix A). Thus, the entries in $\nabla \mathcal{L}(X)$ is bounded and thus $\|\nabla \mathcal{L}(X)\|$ is bounded, i.e., $\|\nabla \mathcal{L}(X)\| \le u_{\mathcal{L}}$.

Denote $H(\cdot)$ as the hessian. Then similarly, we can show that the entities in H(Z), ∇r_{ν} and $H(r_{\nu})$ (see Appendix A) are bounded, i.e., $\|H(Z)\| \le u_Z$, $\|\nabla r_{\nu_i}\| \le u_{r_{\nu}}$ and $\|H(r_{\nu})\| \le u_{r_{\nu}}$, where u_z , $u_{r_{\nu}}$ and $u_{r_{\nu}}$ are positive constants. Denote $\max(r_{\nu_i}) = r_m$ and $\max(\lambda^{\nu_i}) = \lambda$ Then, from Eq.(10), we have

Let $\zeta = u_z + m(cr_m + \lambda)u_{r'_o} + mcu_{r'_o}^2$. By mean value theorem for vector-valued functions, we have:

$$\|\nabla \mathcal{L}(X) - \nabla \mathcal{L}(\bar{X})\| = \|H(\mathcal{L})(X - \bar{X})\| \le \zeta \|X - \bar{X}\|$$

$$\tag{40}$$

O.E.D

Proof of Lemma 7: Recall (18) that $G = \frac{m}{m-s} \nabla \mathscr{F}^T B$, then we could derive ϕ_{D-AL} as follows,

$$\phi_{D-AL} = E(\| \mathbf{G} - \nabla \mathcal{L} \|^{2}) = E\left(\| \frac{m}{m-s} \nabla \mathcal{F}^{T} \mathbf{B} - \nabla \mathcal{F}^{T} \mathbf{1}_{m} \|^{2}\right) \\
\leq E\left(\| \frac{m}{m-s} \mathbf{B} - \nabla \mathcal{F}^{T} \mathbf{1}_{m} \|^{2}\right) \| \nabla \mathcal{F} \|^{2} \\
= \left(E_{s=m}\left(\| \frac{m}{m-s} \mathbf{B} - \mathbf{1}_{m} \|^{2}\right) + E_{s< m}\left(\| \frac{m}{m-s} \mathbf{B} - \mathbf{1}_{m} \|^{2}\right)\right) \| \nabla \mathcal{F} \|^{2}$$
(41)

Where s is the number of disconnected vehicles. Below we process $E_{s=m}$ and $E_{s< m}$ separately.

When s=m (every vehicle is disconnected), we set $\frac{m}{m-s}B=0_m$ as in Lemma 5. Then we have $\|\frac{m}{m-s}B-1_m\|^2=m$ and (42) below.

$$E_{s=m}\left(\left\|\frac{m}{m-s}\mathbf{B}-1_{m}\right\|^{2}\right)=mq^{m}$$
(42)

When s < m, we first have (43) below, given $\mathbf{B} = (b_1, ..., b_m)^T$ and each b_i is either 0 or 1.

$$\mathbf{B}^{T}\mathbf{B} = \sum_{i=1}^{m} b_{i}^{2} = \sum_{i=1}^{m} b_{i} = \mathbf{B}^{T} \mathbf{1}_{m} = m - s, \tag{43}$$

Built upon that, we process $E_{s < m}$ as follows.

$$E_{s < m} \left(\left\| \frac{m}{m - s} \mathbf{B} - \mathbf{1}_{m} \right\|^{2} \right) = E_{s < m} \left(\frac{m^{2}}{(m - s)^{2}} \mathbf{B}^{T} \mathbf{B} + \mathbf{1}_{m}^{T} \mathbf{1}_{m} - \frac{2m}{m - s} \mathbf{B}^{T} \mathbf{1}_{m} \right)$$

$$= E_{s < m} \left(\frac{ms}{m - s} \right)$$

$$= \sum_{s = 0}^{m - 1} \frac{ms}{m - s} C_{m}^{s} q^{s} (1 - q)^{m - s}$$

$$= m \sum_{s = 1}^{m - 1} \frac{m - s + 1}{m - s} \frac{m!}{(m - s + 1)!(s - 1)!} q^{s} (1 - q)^{m - s} \le 2m \sum_{s = 1}^{m - 1} C_{m}^{s - 1} q^{s} (1 - q)^{m - s}$$

$$= 2m \sum_{i = 0}^{m - 2} C_{m}^{i} q^{i + 1} (1 - q)^{m - i - 1}$$

$$= \frac{2mq}{1 - q} \sum_{i = 0}^{m - 2} C_{m}^{i} q^{i} (1 - q)^{m - i} \le \frac{2mq}{1 - q} \sum_{i = 0}^{m} C_{m}^{i} q^{i} (1 - q)^{m - i}$$

$$= \frac{2mq}{1 - q}$$

Inserting (42) and (44) into (41), we could then conclude that

$$\phi_{D-AL} \le m \left(q^m + \frac{2q}{1-q} \right) \| \nabla \mathscr{F} \|^2 \tag{45}$$

Q.E.D

Proof of Lemma 8:

The *i*'th row of $\nabla \mathscr{F} = (\nabla f_{\nu_1}, ..., \nabla f_{\nu_m})^T$ is $\nabla f_{\nu_i} = \left(\frac{\partial f_{\nu_i}}{\partial p_s^{\nu_i \cdot l_1}}, ..., \frac{\partial f_{\nu_i}}{\partial p_s^{\nu_i \cdot l_{\nu_m}}}\right)$. Recall from (15) that $f_{\nu} = \sum_{i=1}^{k_{\nu}} p_s^{\nu_i \cdot l} C_{\nu}^i(P_s) + \frac{1}{2c} \sum_{\nu=1}^m (\max^2\{0, \lambda^{\nu} + cr_{\nu}(X)\} - \lambda^{\nu^2})$

Then, the entities in matrix $\nabla \mathscr{F}$ can be derived as follows.

$$\frac{\partial f_{v^*}}{\partial p_s^{v^*,i}} = \begin{cases} \sum_{l} c_l(f_s^l) \delta_{v^*,i}^{l} + \sum_{L} p_s^{v^*,i} c_l^{'}(f_s^l) \delta_{v^*,i}^{l} + (cr_{v^*} + \lambda^{v^*}) \frac{\partial r_{v^*}}{\partial p_s^{v^*,i}}, & if \quad \lambda^{v^*} + cr_{v^*}(\textbf{\textit{X}}) \leq 0 \\ \sum_{l} c_l(f_s^L) \delta_{v^*,i}^{l} + \sum_{l} p_s^{v^*,i} c_l^{'}(f_s^l) \delta_{v^*,i}^{l}, & if \quad \lambda^{v^*} + cr_{v^*}(\textbf{\textit{X}}) \leq 0 \end{cases}$$

$$\frac{\partial f_{v^{*}}}{\partial p_{s}^{v^{'},i}} = \begin{cases} \sum_{l} p_{s}^{v^{*},i} c_{l}^{'} \left(f_{s}^{l}\right) \delta_{v^{'},i}^{l} \delta_{v^{*},i}^{l} + \left(cr_{v^{*}} + \lambda^{v^{*}}\right) \frac{\partial r_{v^{*}}}{\partial p_{s}^{v^{'},i}}, & \text{if} \quad \lambda^{v^{*}} + cr_{v^{*}}(\textbf{\textit{X}}) > 0 \\ \sum_{l} p_{s}^{v^{*},i} c_{l}^{'} \left(f_{s}^{l}\right) \delta_{v^{'},i}^{l} \delta_{v^{*},i}^{l}, & \text{if} \quad \lambda^{v^{*}} + cr_{v^{*}}(\textbf{\textit{X}}) \leq 0 \end{cases}, \quad \forall v^{'} \neq v^{*}$$

Then similar to the analysis in Lemma 6, all entries in $\nabla \mathscr{T}$ are bounded and thus $\nabla \mathscr{T}$ is bounded, i.e., $\|\nabla \mathscr{T}\| \le u_f$, where u_f is a positive constant. O.E.D

Proof of Theorem 9: using Lemma 5 – Lemma 8, we show how our problem of solving the MP - S of (14) by the process (20) in the D-AL satisfies the assumptions of Theorem 3.

1) Lemma 8 shows that the objective function \mathcal{L} of MP-S in (14) satisfies the ζ Lipschitz continuous requirement in Theorem 3, i.e.,

$$\| \nabla \mathcal{L}(\mathbf{X}) - \nabla \mathcal{L}(\bar{\mathbf{X}}) \| \leq \zeta \| \mathbf{X} - \bar{\mathbf{X}} \|$$

2) Set $d_t = \nabla \mathcal{L}$, $\omega_t = G - \nabla \mathcal{L}$, $c_1 = c_2 = 1$, then assumption (a) of Theorem 3 is satisfied, i.e.,

$$\|\nabla \mathcal{L}(\mathbf{X})\|^{2} \leq \nabla \mathcal{L}(\mathbf{X})^{T} \nabla \mathcal{L}(\mathbf{X}), \quad \|\nabla \mathcal{L}\| \leq 1 + \|\nabla \mathcal{L}\| \|\forall k,$$

3) Set $c_3 = \sigma = 1 - q^m$, Lemma 5 shows that the assumption (b) of Theorem 3 is satisfied, i.e.,

$$E(\mathbf{G}) = \sigma \nabla \mathscr{L} \ \forall k$$

4) Combining Lemma 6 – 8, for any positive constant $A \ge \frac{mqu_f^2}{(1-q)(1+u_r^2)}$, assumption (c) of Theorem 3 is satisfied, i.e.

$$E(\parallel \mathbf{G} - \nabla \mathcal{L} \parallel^2) \leq A(1 + \parallel \nabla \mathcal{L}(\mathbf{X}) \parallel^2)$$

Assumption (d) of Theorem 3 is the standard step size assumption, which can be satisfied by any diminishing step size rule. Together these indicate that the MP - S in our problem and the D-AL algorithm under communication failures satisfy the assumptions in Theorem 3. Thus, using the D-AL to solve the MP - S of (14) will guarantee the solution converge to a first-order optimality solution, and consequently the original problem of the MP in (8.1) – (8.5) will converge to a local solution under random vehicle communication failures. Q.E.D

Appendix E

Proof of Theorem 10:

Denote $\omega_k = G_k - \nabla \mathscr{L}_k$ and $\phi = E(\|\omega_k\|^2)$ at iteration k. Since the gradient of \mathscr{L} (the objective function of the MP - S (14)) is ζ Lipschitz continuous (Lemma 6), we have that

$$\mathscr{L}(X_{k+1}) \le \mathscr{L}(X_k) + \nabla \mathscr{L}^T(X_{k+1} - X_k) + \frac{\zeta}{2} ||X_{k+1} - X_k||^2$$
(46)

Substituting (20) into (46), we have

$$\mathcal{L}(\boldsymbol{X}_{k+1}) \leq \mathcal{L}(\boldsymbol{X}_{k}) - \nabla \mathcal{L}_{k}^{T} \alpha_{k} \boldsymbol{G}_{k} + \frac{\zeta}{2} \| \alpha^{k} \boldsymbol{G}_{k} \|^{2}$$

$$= \mathcal{L}(\boldsymbol{X}_{k}) - \alpha_{k} \nabla \mathcal{L}_{k}^{T} (\boldsymbol{\omega}_{k} + \nabla \mathcal{L}_{k}) + \frac{\zeta}{2} \| \alpha_{k}^{2} \boldsymbol{\omega}_{k} + \nabla \mathcal{L}_{k} \|^{2} =$$

$$\mathcal{L}(\boldsymbol{X}_{k}) - \alpha_{k} \nabla \mathcal{L}_{k}^{T} \boldsymbol{\omega}_{k} - \| \alpha_{k} \nabla \mathcal{L}_{k} \|^{2}$$

$$+ \frac{\zeta}{2} \alpha_{k}^{2} (\| \nabla \mathcal{L}_{k} \|^{2} + \| \boldsymbol{\omega}_{k} \|^{2} + 2 \nabla \mathcal{L}_{k}^{T} \boldsymbol{\omega}_{k})$$

$$= \mathcal{L}(\boldsymbol{X}_{k}) - \left(\alpha_{k} - \frac{\zeta}{2} \alpha_{k}^{2}\right) \| \nabla \mathcal{L}_{k} \|^{2} - \left(\alpha_{k} - \zeta \alpha_{k}^{2}\right) \nabla \mathcal{L}_{k}^{T} \boldsymbol{\omega}_{k}$$

$$+ \frac{\zeta}{2} \alpha_{k}^{2} \| \boldsymbol{\omega}_{k} \|^{2}$$

$$(47)$$

Reorganizing (47), we have:

$$\left(\alpha_{k} - \frac{\zeta}{2}\alpha_{k}^{2}\right) \|\nabla \mathcal{L}_{k}\|^{2} \leq \mathcal{L}(X_{k}) - \mathcal{L}(X_{k+1}) - \left(\alpha_{k} - \zeta\alpha_{k}^{2}\right) \nabla \mathcal{L}_{k}^{T} \omega_{k} + \frac{\zeta}{2}\alpha_{k}^{2} \|\omega_{k}\|^{2}$$

$$(48)$$

Summing up (48) from k = 0, ..., N - 1, where N is the first iteration that satisfies $\nabla \mathscr{L}_N^2 \leq \varepsilon$, we have:

$$\sum_{k=0}^{N-1} \left(\alpha_k - \frac{\zeta}{2} \alpha_k^2 \right) \| \nabla \mathcal{L}_k \|^2 \le \mathcal{L}(X_0) - \mathcal{L}(X_N) - \sum_{k=1}^{N} \left(\alpha_k - \zeta \alpha_k^2 \right) \nabla \mathcal{L}_k^T \omega_k + \frac{\zeta}{2} \sum_{k=1}^{N} \alpha_k^2 \| \omega_k \|^2$$

$$\tag{49}$$

Note that $\|\nabla \mathcal{L}_N\|^2 \le \varepsilon \le \|\nabla \mathcal{L}\|_k^2$, k = 1, ..., N-1, we thus have:

$$\sum_{k=0}^{N-1} \left(\alpha_k - \frac{\zeta}{2} \alpha_k^2 \right) \| \nabla \mathcal{L}_N \|^2 \le \mathcal{L}(X_0) - \mathcal{L}(X_N) - \sum_{k=1}^{N} \left(\alpha_k - \zeta \alpha_k^2 \right) \nabla \mathcal{L}_k^T \omega_k + \frac{\zeta}{2} \sum_{k=1}^{N} \alpha_k^2 \| \omega_k \|^2$$

$$(50)$$

From Remark 4 and Lemma 5, G_k in our problem could be seen as an unbiased estimator of $\nabla \mathcal{L}_k$, i.e., $E(G_k) = \nabla \mathcal{L}_k$ Thus:

$$E(\nabla \mathcal{L}_k^T \omega_k) = E(\nabla \mathcal{L}_k^T (G_k - \nabla \mathcal{L}_k)) = 0$$
(51)

Then, taking the expectation of (50) and incorporating (51), we have:

$$\sum_{k=0}^{N-1} \left(\alpha_k - \frac{\zeta}{2} \alpha_k^2 \right) E\left(\| \nabla \mathcal{L}_N \|^2 \right) \le \mathcal{L}(X_0) - \mathcal{L}(X_N) + \frac{\zeta}{2} \sum_{k=1}^{N} \alpha_k^2 \phi$$
(52)

If the step size is set to be a constant of $\frac{1}{\zeta\sqrt{N}}$ i.e., $\alpha_k = \frac{1}{\zeta\sqrt{N}}$, then $\alpha_k - \frac{\zeta}{2}\alpha_k^2 = \frac{2\sqrt{N}-1}{2\zeta N} > 0$. Then from (52), we have:

$$E(\|\nabla \mathscr{L}_N\|^2) \le \frac{2\zeta(\mathscr{L}(X_0) - \mathscr{L}(X_N)) + \phi}{2\sqrt{N} - 1} \le \frac{2\zeta(\mathscr{L}(X_0) - \mathscr{L}(X_N)) + \phi}{\sqrt{N}}$$

$$(53)$$

Then, to ensure $E(\|\nabla \mathcal{L}_N\|^2) \le \varepsilon$, it suffices to have

$$\frac{2\zeta(\mathscr{L}(X_0) - \mathscr{L}(X_N)) + \phi}{\sqrt{N}} = \varepsilon \tag{54}$$

Which vields

$$N = \frac{\left(2\zeta(\mathscr{L}(X_0) - \mathscr{L}(X_N)\right) + \phi\right)^2}{\varepsilon^2} \tag{55}$$

Omitting constant terms in (55), we have that the convergence complexity to reach certain solution accuracy ε is $O(N) = O\left(\frac{\psi^2}{\varepsilon^2}\right)$. Q.E.D Proof of Corollary 11:

From Lemma 7 and Lemma 8, we have that $\phi_{D-AL} = E(\|G - \nabla \mathcal{L}\|^2) \le m \left(q^m + \frac{2}{1-q} - 2\right) u_f^2$. We could then reach the relation by inserting ϕ_{D-AL} to (55) and omitting constant i.e., m, ζ , $\mathcal{L}(X_0)$, $\mathcal{L}(X_N)$, u_f , and high order terms, i.e., q^m .

Appendix F

Proof of Lemma 12:

From (21), we have

$$\phi_{aD-AL} = E\left(\|\mathbf{G}_{a} - \nabla \mathcal{L}\|^{2}\right)$$

$$= E\left(\|\frac{m}{(m-s)d}\nabla \mathcal{F}^{T}\mathbf{W}\mathbf{1}_{m-s} - \nabla \mathcal{F}^{T}\mathbf{1}_{m}\|^{2}\right) \leq E\left(\|\frac{m}{(m-s)d}\mathbf{W}\mathbf{1}_{m-s} - \mathbf{1}_{m}\|^{2}\right)\|\nabla \mathcal{F}\|$$

$$= \left(E_{s=m}\left(\|\frac{m}{(m-s)d}\mathbf{W}\mathbf{1}_{m-s} - \mathbf{1}_{m}\|^{2}\right) + E_{s< m}\left(\|\frac{m}{(m-s)d}\mathbf{W}\mathbf{1}_{m-s} - \mathbf{1}_{m}\|^{2}\right)\right)\|\nabla \mathcal{F}\|^{2}$$

$$(56)$$

Simillar to the discussions in Lemma 5 and 7, when s=m, i.e., when every vehicle is disconnected, the CP receives no information and let $\frac{m}{(m-s)d}W1_{m-s}=0_m$. Then, for s=m, we have

$$E_{s=m}\left(\|\frac{m}{(m-s)d}W1_{m-s}-1_{m}\|^{2}\right)=mq^{m}$$
(57)

For s < m, we have

$$E_{s < m} \left(\left\| \frac{m}{(m - s)d} \mathbf{W} \mathbf{1}_{m - s} - \mathbf{1}_{m} \right\|^{2} \right)$$

$$= E_{s < m} \left(\frac{m^{2}}{(m - s)^{2} d^{2}} \mathbf{1}_{m - s}^{T} \mathbf{W}^{T} \mathbf{W} \mathbf{1}_{m - s} + \mathbf{1}_{m}^{T} \mathbf{1}_{m} - \frac{2m}{(m - s)d} \mathbf{1}_{m}^{T} \mathbf{W} \mathbf{1}_{m - s} \right)$$
(58)

Note that the number of 1s in every column of W is d, we thus have,

Let A_i denote the i'th column of A. Note that the assignment plan defined by assignment matrix A can also be considered as assigning every computation task to d vehicles, then for $i \neq j$, we have

$$\sum_{i=1}^{m} \sum_{j=1}^{m/i} A_i^T A_j = md(d-1)$$
 (60)

Denote the i'th column of the $m \times (m-s)$ matrix \mathbf{W} as W_i . To be noted, \mathbf{W} is a random matrix associated with the random variable $s = m - \sum_{i=1}^{m} b_i$ and $\mathbf{b}_i = 1$ with probability 1 - q, indicating vehicle v_i is connected. The column W_i of \mathbf{W} is taken from \mathbf{A} when the corresponding vehicle v_i is well connected, i.e., $b_i = 1$. Also, note that the disconnection probabilities are independent between vehicles. Then, we have the results below.

For i = j, $W_i^T W_i = d$ since each vehicle is assigned d computation tasks.

For $i \neq j$, using (60), given the number of disconnected vehicles s, we have the derivation as follows.

$$E_{i\neq j}\left(\sum_{i=1}^{(m-s)}\sum_{j=1}^{(m-s)/i}W_{i}^{T}W_{j}\right)$$

$$=\sum_{m=1}^{m}\sum_{j=1}^{m/i}A_{i}^{T}A_{j}p\left(b_{i}=1,b_{j}=1|s\right)$$

$$=md(d-1)\frac{C_{m-2}^{m-s-2}(q^{s}(1-q)^{m-s})(1-q)^{2}}{C_{m}^{m-s}q^{s}(1-q)^{m-s}}$$

$$=md(d-1)\frac{(m-2)!}{(m-s-2)!s!}\frac{(m-s)!s!}{m!}$$

$$=(m-s)(m-s-1)\frac{d(d-1)}{m-1}$$
(61)

Thus, we have

$$E\left(1_{m-s}^{T}W^{T}W1_{m-s}\right) = E\left(\sum_{i=1}^{m-s}\sum_{j=1}^{m-s}W_{i}^{T}W_{j}\right) = \sum_{i=1}^{m-s}W_{i}^{T}W_{i} + E_{i\neq j}\left(\sum_{i=1}^{m-s}\sum_{j=1}^{m-s/i}W_{i}^{T}W_{j}\right) = (m-s)d + (m-s)(m-s-1)\frac{d(d-1)}{m-1}$$
(62)

Insert (59) and (62) to (58), we have

$$E_{s < m} \left(\left\| \frac{m}{(m-s)d} W \mathbf{1}_{m-s} - \mathbf{1}_{m} \right\|^{2} \right)$$

$$= E_{s < m} \left(\frac{m^{2}}{(m-s)^{2} d^{2}} \left((m-s)d + (m-s)(m-s-1) \frac{d(d-1)}{m-1} \right) + m - \frac{2m}{(m-s)d} d(m-s) \right)$$

$$= E_{s < m} \left(\frac{ms(m-d)}{(m-s)d(m-1)} \right)$$
(63)

Since the number of tasks assigned to each vehicle $d \ge 1$, we then have

$$E_{s < m} \left(\frac{ms(m-d)}{(m-s)d(m-1)} \right) = \sum_{s=0}^{m-1} \frac{ms(m-d)}{(m-s)d(m-1)} C_m^s q^s (1-q)^{m-s}$$

$$\leq \sum_{s=0}^{m-1} \frac{ms(m-1)}{(m-s)d(m-1)} C_m^s q^s (1-q)^{m-s}$$

$$= \sum_{s=0}^{m-1} \frac{ms}{(m-s)d} C_m^s q^s (1-q)^{m-s}$$

$$= \frac{m}{d} \sum_{s=1}^{m-1} \frac{m-s+1}{m-s} \frac{m!}{(m-s+1)!(s-1)!} q^s (1-q)^{m-s}$$

$$\leq \frac{2m}{d} \sum_{s=1}^{m-1} C_m^{s-1} q^s (1-q)^{m-s}$$

$$= \frac{2m}{d} \sum_{i=0}^{m-2} C_m^i q^{i+1} (1-q)^{m-i-1}$$

$$= \frac{2mq}{(1-q)d} \sum_{i=0}^{m-2} C_m^i q^i (1-q)^{m-i}$$

$$\leq \frac{2mq}{(1-q)d} \sum_{i=0}^{m} C_m^i q^i (1-q)^{m-i}$$

$$= \frac{2mq}{(1-q)d} \sum_{i=0}^{m} C_m^i q^i (1-q)^{m-i}$$

$$= \frac{2mq}{(1-q)d} \sum_{i=0}^{m} C_m^i q^i (1-q)^{m-i}$$

$$= \frac{2mq}{(1-q)d} \sum_{i=0}^{m} C_m^i q^i (1-q)^{m-i}$$

Combining (57) and (64) to (56), we could reach the conclusion: $\phi_{aD-AL} \leq \left(mq^m + \frac{2mq}{(1-\alpha)d}\right) \|\nabla \mathcal{F}\|^2$. Q.E.D

Appendix G

Lemma 14. The time complexity to solve the CeRM problem under the D-AL solution algorithm is of $O\left(k^2m^2\varepsilon_1^{\frac{2}{\gamma_c-1}}\varepsilon_2^{-2}\right)$, where k is the number of candidate paths for each vehicle, m is the number of vehicles, ε_1 and ε_2 is the solution accuracy parameter for the original problem (Eq. (8.1) – (8.5)) and the sub-problem (MP-AL of Eq. (11)) respectively, i.e., $E(\|\nabla Z_{\mathscr{L}}\|^2) \le \varepsilon_1$ and $E(\|\nabla \mathscr{L}\|^2) \le \varepsilon_2$, where $Z_{\mathscr{L}}(X, \lambda_K) = \sum_{L=1}^n f_s^L c_L(f_s^L) - \sum_{\nu=1}^m \lambda_K^\nu r_\nu(X)$ is the Lagrangian function of the original problem and \mathscr{L} is the objective function of MP-AL.

Proof: Note that our distributed solution algorithm D-AL is built upon the Augmented Lagrangian method (transform the original problem to solving and updating MP-AL of Eq. (11) iteratively, **outer iteration**) and the projected gradient descent method (solving an MP-AL of Eq. (11), **inner iteration**). It has been shown by (Grapiglia et al., 2021) that the complexity of outer iterations of the Augmented Lagrangian method only relates to the solution accuracy parameter ε (ε -approximate solution), i.e., $O\left(\varepsilon_1^{-\frac{2}{\kappa^{c-1}}}\right)$, where γ_c controls how fast the penalty parameter increases as shown in Table 1 Parameter updating scheme on page 13 in our manuscript. In addition, as we have proved in Theorem 10, the complexity of inner iterations is $O(\varepsilon_2^{-2})$ given constant approximation errors. The complexity of inner iteration only relates to the solution accuracy parameter ε_2 . With that said, the complexity of the total number of iterations (the number of outer iterations multiplies the number of inner iterations) is of $O\left(\varepsilon_1^{-\frac{2}{\kappa_1-1}}\varepsilon_2^{-2}\right)$.

Next, we analyze the time complexity for each vehicle to complete its assigned computation load under D-AL in one inner iteration. Assuming that each vehicle has k candidate paths and there are m participating vehicles, as we have shown in the proof of Theorem 1, the time complexity of each vehicle to complete its assigned computation load under D-AL in one iteration is (km+1)l, where l is the time complexity to numerically evaluate the value of f_V (the individual vehicle v's augmented objective function, see Eq. (14)). From the formulation of f_V , i.e., $f_V = \sum_{i=1}^{k_v} p_S^{v,i} C_V^i(P_S) + \frac{1}{2c} \sum_{\nu=1}^m (\max^2\{0, \lambda^{\nu} + cr_V(X)\} - \lambda^{\nu 2})$, we can know that l has a linear relation with the number of candidate path k and the number of vehicles m, i.e., O(km). Thus, we can conclude that the time complexity of each vehicle to complete its assigned computation load under D-AL in one iteration has a quadratic relation with the number of candidate path k and the number of vehicles m, i.e., $O((km+1)l) = O(k^2m^2)$.

Combining the above discussion, we can conclude that the time complexity to solve the CeRM problem using the D-AL solution algorithm is of $O\left(k^2m^2\varepsilon_1^{-\frac{2}{\kappa-1}}\varepsilon_2^{-2}\right)$. Given the solution accuracy requirement, the time complexity will have a quadratic relation with the number of vehicles m and the number of candidate paths k for each vehicle.

Appendix H

Independent Routing (IR)

In an independent routing mechanism, each individual driver independently does the best response to the real-time traffic conditions. In this study, we adopt the commonly used multinomial logit-based (MNL) behavior choice model. According to the real-time traffic information $C^i_{\nu,o}$, individual vehicle's independent routing choice preference could then be calculated by the MNL model:

$$p^{v,i} = rac{e^{-V_{v,i}}}{\sum_{i=1}^{k_v} e^{-V_{v,i}}},$$

where

$$V_{v,i} = \alpha^v + \beta^v C_v^i,$$

is the measured utility of route r_{ν}^{i} for vehicle ν and α^{ν} , β^{ν} are vehicle-specific constant scalars representing the characteristics of each individual. Readers can refer to Sec 3.1 for a detailed introduction.

user-oriented Equilibrium Routing (uoER)

There are several approaches to derive an uoER. Under the assumption of logit-choice model, this study adopts the coordinated routing mechanism proposed in (Du, Han, and Li, 2014). Specifically, the route preference is calculated by:

$$\min_{p} \sum_{l \in \mathcal{L}} \int_{0}^{f_{l}} c_{l}(w) dw + \sum_{v=1}^{m} \sum_{i=1}^{k^{v}} \frac{1}{\beta_{v}} p^{v,i} \ln(p^{v,i})$$

$$\begin{split} &\sum_{i=1}^{k_{v}} p^{v,i} = 1, \ \forall v = 1, ..., m \\ &\sum_{i=1}^{k_{v}} p^{v,i} = 1, \ \forall v = 1, ..., m \\ &f_{l} = \sum_{i=1}^{m} \sum_{j=1}^{k^{v}} p^{v,i} \delta_{v,i}^{L}, \ \forall l \in L \end{split}$$

And the corresponding system cost is calculated by $C_{\text{sys}} = \sum_{l=1}^{n} f_l c_l(f_s^l)$.

System Optimum Routing (SOR)

We consider there is a centralized agent to systemically generate the route preference for each driver, aiming to minimize the expected system travel cost C_{Sys} . Then the SOR routing preference could be calculated by solving the following:

$$\min_{p} C_{sys} = \sum_{l=1}^{n} f_l c_l(f_l)$$

s.t

$$\begin{split} &\sum_{i=1}^{k_{v}} p^{v,i} = 1, \ \forall v = 1, ..., m \\ &p^{v,i} \ge 0, \ \forall v = 1, ..., m, \ \forall \ i = 1, ..., k' \\ &f_{l} = \sum_{v=1}^{m} \sum_{i=1}^{k^{v}} p^{v,i} \delta_{v,i}^{L}, \quad \forall l \in L \end{split}$$

To be noted, the agent generates route choice probability not a route choice for individual vehicles to make it consistent to the setup of our CeRM in this study.

Appendix I

Topologies of Sioux Falls Fig. 15 and EMA network Fig. 16.

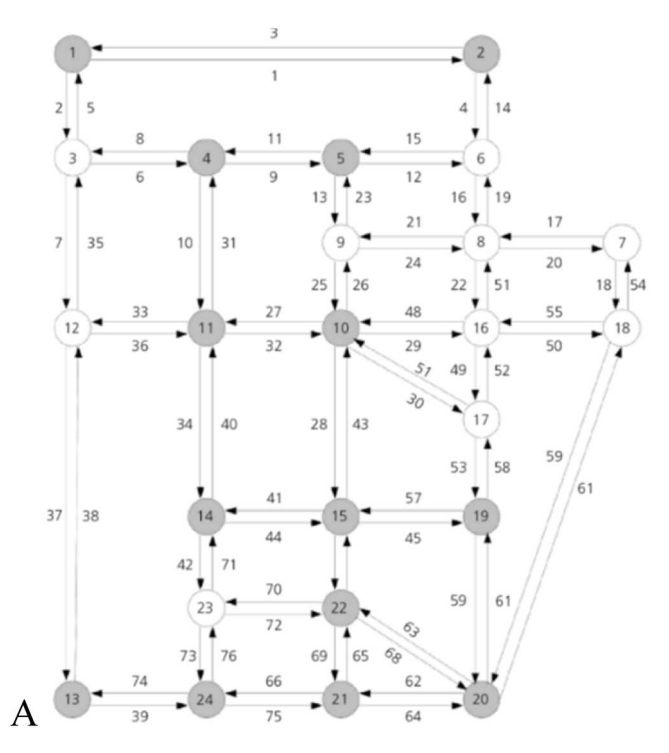


Fig. 15. Sioux Falls city network.

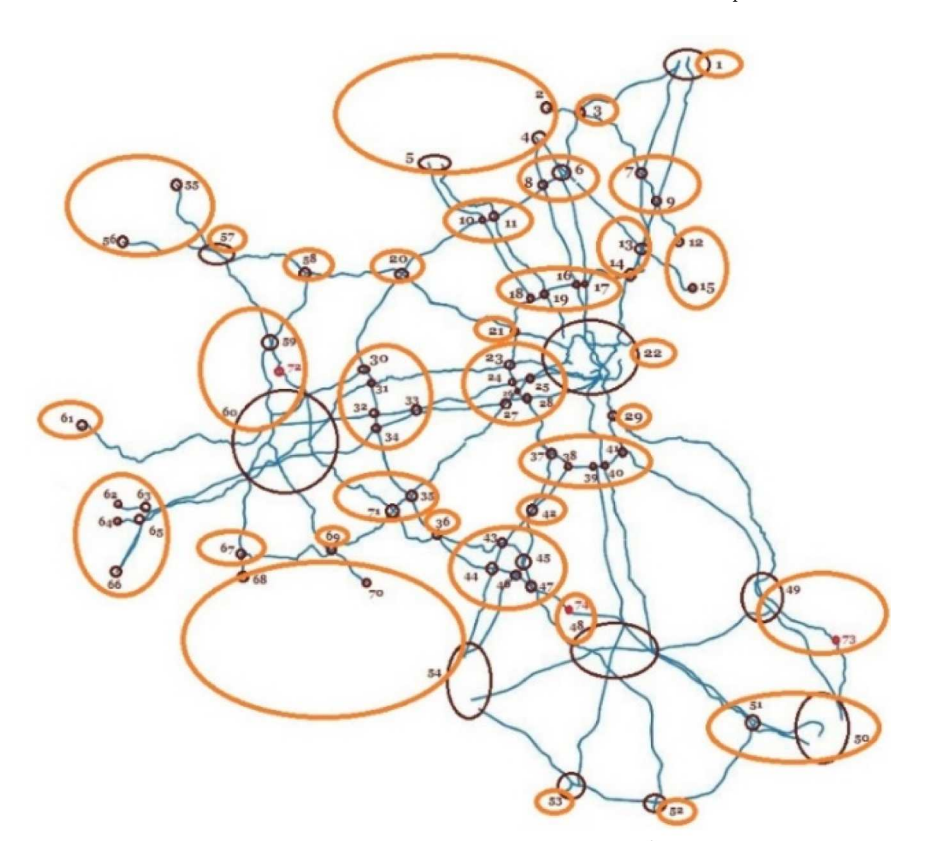


Fig. 16. EMA network.

References

Orange County Traffic Counts. Orange County Government. https://www.orangecountyfl.net/Portals/0/Resource%20Library/traffic%20-%20transportation/traffic %20count%20reports/2020%20Printable%20Report ALL.pdf.

Ben-Akiva, Moshe, Palma, Andre De, Isam, Kaysi, 1991. Dynamic network models and driver information systems. General 25 (5), 251–266.

Bertsekas, Dimitri P., 1997. Nonlinear programming. J. Oper. Res. Soc. 48 (3), 334. -334.

Bertsekas, Dimitri P., Tsitsiklis, John N., 2000. Gradient convergence in gradient methods with errors. SIAM J. Optim. 10 (3), 627-642.

Boggs, Paul T., Tolle, Jon W., 1995. Sequential quadratic programming. Acta Numer. 4, 1–51.

Bottou, Léon, Curtis, Frank E., Nocedal, Jorge, 2018. Optimization methods for large-scale machine learning. SIAM Rev. 60 (2), 223–311.

Chen, Yunmei, Ye, Xiaojing, 2011. Projection onto a simplex. arXiv preprint arXiv:1101.6081.

Cormen, Thomas H., et al., 2009. Introduction to algorithms. MIT press.

Das, Sanmay, Kamenica, Emir, Mirka, Renee, 2017. Reducing congestion through information design. In: 2017 55th annual Allerton conference on communication, control, and computing (Allerton). IEEE.

de Palma, André, Lindsey, Robin, 2011. Traffic congestion pricing methodologies and technologies. Emerging Technologies 19 (6), 1377-1399.

Du, Lili, Chen, Shuwei, Han, Lanshan, 2015. Coordinated online in-vehicle navigation guidance based on routing game theory. Transp. Res. Rec. 2497 (1), 106–116. Du, Lili, Han, Lanshan, Chen, Shuwei, 2015. Coordinated online in-vehicle routing balancing user optimality and system optimality through information perturbation. Methodological 79, 121–133.

Du, Lili, Han, Lanshan, Li, Xiang-Yang, 2014. Distributed coordinated in-vehicle online routing using mixed-strategy congestion game. Methodological 67, 1–17. Gairing, Martin, Monien, Burkhard, Tiemann, Karsten, 2008. Selfish routing with incomplete information. Theory Comput Syst 42 (1), 91–130.

Ghadimi, Saeed, Lan, Guanghui, 2013. Stochastic first-and zeroth-order methods for nonconvex stochastic programming. SIAM J. Optim. 23 (4), 2341–2368.

Grzybek, Agata, et al., 2015. Mitigating flash crowd effect using connected vehicle technology. Vehicular Communications 2 (4), 238–250.

Guo, Xiaolei, Yang, Hai, 2010. Pareto-improving congestion pricing and revenue refunding with multiple user classes. Methodological 44 (8-9), 972–982.

Hess, Stephane, Bierlaire, Michel, Polak, J., 2004. Estimation of value-of-time using Mixed Logit models. No. REP_WORK.

Iusem, Alfredo N., 2003. On the convergence properties of the projected gradient method for convex optimization. Recent Adv. Appl. Biomed. Inf. Comput. Eng. Syst. Appl., Proc. 11th WSEAS Int. Conf. Appl. Inf. Commun. (AIC '11); Proc. 4th WSEAS Int. Conf. Biomed. Electron. Biomed. Inf. (BEBI '11); Proc. Int. Conf. Environ., Econ., Energy, Devices, Syst., Commun., Comput., Pure Appl. Math. 22, 37–52.

Jung, Taeho, et al., 2013. Privacy-preserving data aggregation without secure channel: Multivariate polynomial evaluation. In: 2013 Proceedings IEEE INFOCOM. IEEE.

Klein, Ido, Levy, Nadav, Ben-Elia, Eran, 2018. An agent-based model of the emergence of cooperation and a fair and stable system optimum using ATIS on a simple road network. Emerging Technologies 86, 183–201.

Koutsoupias, Elias, Papadimitriou, Christos, 1999. Worst-case equilibria. In: Annual symposium on theoretical aspects of computer science. Springer, Berlin, Heidelberg.

Lam, Terence C., Small, Kenneth A., 2001. The value of time and reliability: measurement from a value pricing experiment. ogistics and Transportation Review 37 (2-3), 231–251.

Lessan, Javad, Fu, Liping, 2019. Credit-and permit-based travel demand management state-of-the-art methodological advances. Transport Science 1–24. Liu, Jeffrey, Amin, Saurabh, Schwartz, Galina, 2016. Effects of information heterogeneity in Bayesian routing games. arXiv preprint arXiv:1603.08853.

Liu, Yixuan, Whinston, Andrew B., 2019. Efficient real-time routing for autonomous vehicles through bayes correlated equilibrium: An information design framework. Information Economics and Policy 47, 14-26.

Lotfi, Mohammad Hassan, La, Richard J., Martins, Nuno C., 2018. Bayesian Congestion Game with Traffic Manager: Binary Signal Case. In: 2018 IEEE Conference on Decision and Control (CDC). IEEE.

Ma, Jiaqi, Smith, Brian L., Zhou, Xuesong, 2016. Personalized real-time traffic information provision: Agent-based optimization model and solution framework. Emerging Technologies 64, 164-182.

Mahajan, Niharika, et al., 2019. Design analysis of a decentralized equilibrium-routing strategy for intelligent vehicles. Emerging Technologies 103, 308–327.

Menelaou, C., et al., 2017. Controlling road congestion via a low-complexity route reservation approach. Emerging Technologies 81, 118-136.

Menelaou, Charalambos, et al., 2018. Minimizing traffic congestion through continuous-time route reservations with travel time predictions. IEEE Transactions on Intelligent Vehicles 4 (1), 141–153.

Mongin, Philippe., 1998. Expected utility theory.

Morandi, Valentina., 2021. Bridging the user equilibrium and the system optimum in static traffic assignment; how the cooperation among drivers can solve the congestion problem in city networks. arXiv preprint arXiv:2105.05804.

Nemirovski, Arkadi, et al., 2009. Robust stochastic approximation approach to stochastic programming. SIAM J. Optim. 19 (4), 1574-1609.

Nuzzolo, Agostino, Comi, Antonio, 2016. Individual utility-based path suggestions in transit trip planners. IET Intel. Transport Syst. 10 (4), 219-226.

Papadopoulos, Aristotelis-Angelos, et al., 2021. Personalized Pareto-improving pricing-and-routing schemes for near-optimum freight routing: An alternative approach to congestion pricing. Emerging Technologies 125, 103004.

Peng, Wang, Du, Lili, 2021. Forming coordination group for coordinated traffic congestion management schemes. Emerging Technologies 128, 103113.

Peng, Wang, Du, Lili, 2022. Investigating Optimal Carpool Scheme by a Semi-Centralized Ride-Matching Approach. IEEE Trans. Intell. Transp. Syst.

Raviv, Netanel, et al., 2020. Gradient coding from cyclic MDS codes and expander graphs. IEEE Trans. Inf. Theory 66 (12), 7475-7489.

Reddi, Sashank J., et al., 2016. Stochastic variance reduction for nonconvex optimization. In: International conference on machine learning. PMLR.

Rey, David, et al., 2016. An endogenous lottery-based incentive mechanism to promote off-peak usage in congested transit systems. Transport Policy 46, 46-55. Roughgarden, Tim., 2005. Selfish routing and the price of anarchy. MIT press.

Sheffi, Yosef., 1985. Urban transportation networks, 6. Prentice-Hall, Englewood Cliffs, NJ.

Simon, Herbert A., 1955. A behavioral model of rational choice. Q. J. Econ. 69 (1), 99-118.

Small, Kenneth A., Rosen, Harvey S., 1981. Applied welfare economics with discrete choice models. Econometrica 105-130.

Spana, Stephen, Du, Lili, Yin, Yafeng, 2021. Strategic Information Perturbation for an Online In-Vehicle Coordinated Routing Mechanism for Connected Vehicles Under Mixed-Strategy Congestion Game. IEEE Trans. Intell. Transp. Syst.

Tavafoghi, Hamidreza, Teneketzis, Demosthenis, 2017. Informational incentives for congestion games. In: 2017 55th Annual Allerton Conference on Communication, Control, and Computing (Allerton). IEEE.

Van Amelsfort, Dirk, Bliemer, Michiel, 2005. Valuation of uncertainty in travel time and arrival time-some findings from a choice experiment.

van Essen. Mariska, et al., 2016. From user equilibrium to system optimum: a literature review on the role of travel information, bounded rationality and non-selfish behaviour at the network and individual levels. Transport reviews 36 (4), 527-548.

Wang, Weiran, Carreira-Perpinán, Miguel A., 2013. Projection onto the probability simplex: An efficient algorithm with a simple proof, and an application. arXiv preprint arXiv:1309.1541.

Wu, Di, Yin, Yafeng, Lawphongpanich, Siriphong, 2011. Pareto-improving congestion pricing on multimodal transportation networks. Eur J Oper Res 210 (3), 660-669

Yang, Hai., 1999. System optimum, stochastic user equilibrium, and optimal link tolls. Transportation Science 33 (4), 354-360.

Yen, Jin Y., 1971. Finding the k shortest loopless paths in a network. Management Science 17 (11), 712-716.

Zhang, Lihui, et al., 2014. Solving a discrete multimodal transportation network design problem. Emerging Technologies 49, 73-86.

Zhou, Bo, et al., 2020. A reinforcement learning scheme for the equilibrium of the in-vehicle route choice problem based on congestion game. Appl. Math. Comput. 371, 124895.